RSC Chemical Biology

ROYAL SOCIETY OF CHEMISTRY

PAPER

View Article Online
View Journal | View Issue

Cite this: *RSC Chem. Biol.*, 2024, 5, 1147

Bispecific FpFs: a versatile tool for preclinical antibody development†

Matthew Collins,‡[a] Nkiru Ibeanu,‡[bc] Wiktoria Roksana Grabowska,[d] Sahar Awwad,[bc] Peng T. Khaw,[c] Steve Brocchini [b] and Hanieh Khalili *[bd]

We previously described FpFs **1** (Fab–PEG–Fab) as binding mimetics of IgGs. FpFs are prepared with di(bis-sulfone) conjugation reagents **3** that undergo disulfide rebridging conjugation with the accessible disulfide of each Fab (Scheme 1). We have now prepared bispecific FpFs **2** (bsFpF and Fab_1–PEG–Fab_2) as potential bispecific antibody mimetics with the intent that bsFpFs could be used in preclinical antibody development since sourcing bispecific antibodies may be challenging during preclinical research. The di(bis-sulfone) reagent **3** was first used to prepare a bsFpF **2** by the sequential conjugation of a first Fab and then a second Fab to another target (Scheme 2). Seeking to improve bsFpF synthesis, the asymmetric conjugation reagent, bis-sulfone bis-sulfide **16**, with different thiol conjugation reactivities at each terminus (Scheme 4) was examined and the bsFpFs appeared to be formed at similar conversion to the di(bis-sulfone) reagent **3**. To explore the advantages of using common intermediates in the preparation of bsFpF families, we investigated bsFpF synthesis with a protein conjugation–ligation approach (Scheme 5). Reagents with a bis-sulfone moiety for conjugation on one PEG terminus and a ligation moiety on the other terminus were examined. Bis-sulfone PEG *trans*-cyclooctene (TCO) **28** and bis-sulfone PEG tetrazine (Tz) **30** were used to prepare several bsFpFs targeting various therapeutic targets (TNF-α, IL6R, IL17, and VEGF) and tissue affinity targets (hyaluronic acid and collagen II). Surface plasmon resonance (SPR) binding studies indicated that there was little difference between the dissociation rate constant (k_d) for the unmodified Fab, mono-conjugated PEG–Fab and the corresponding Fab in a bsFpF. The Fab association rate (k_a) in the bsFpF was slower than for PEG–Fab, which may be because of mass differences that influence SPR results. These observations suggest that each Fab will bind to its target independently of the other Fab and that bsFpF binding profiles can be estimated using the corresponding PEG–Fab conjugates.

Received 18th June 2024,
Accepted 8th September 2024

DOI: 10.1039/d4cb00130c

rsc.li/rsc-chembio

Introduction

We previously described an antibody mimetic that is called FpF (Fab–PEG–Fab) **1**, where a poly(ethylene glycol) (PEG) linker mimics the IgG hinge.[1,2] The IgG hinge enables flexibility of the two antigen-binding fragments (Fabs) to provide enhanced binding that can be derived from bivalency to facilitate rebinding to slow dissociation rates.[3,4] The hinge region comprises single polypeptide chains that can be susceptible to degradation.[5] FpFs **1** (structures 1) share comparable solution sizes, binding characteristics,[1] functional activity[2] and enhanced stability[6] with IgG antibodies using PEG linkers with molecular weights in the range of 5–20 kDa. FpFs were designed to maintain the Fab topology and flexibility that has evolved in IgG antibodies with increased stability by substituting the hinge region with a PEG linker that has been stably covalently conjugated to each Fab. With these characteristics of FpFs **1** in mind, we decided to examine the synthesis and binding properties of bispecific antibody mimetics called bsFpFs **2** (Fab_1–PEG–Fab_2).

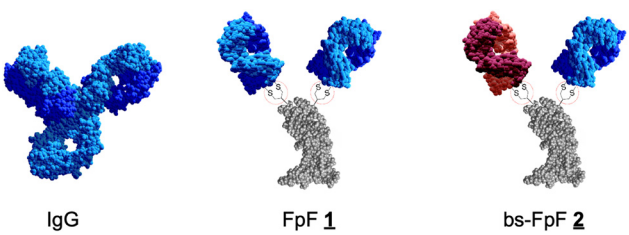

[a] *School of Health, Sport and Bioscience, University of East London, London, UK*
[b] *School of Pharmacy, University College London, London, UK. E-mail: hanieh.khalili@uwl.ac.uk*
[c] *National Institute for Health Research (NIHR) Biomedical Research Centre at Moorfields Eye Hospital NHS Foundation Trust and UCL Institute of Ophthalmology, London EC1V 9EL, UK*
[d] *School of Biomedical Science, University of West London, London, W5 5RF, UK*

† Electronic supplementary information (ESI) available. See DOI: https://doi.org/10.1039/d4cb00130c

‡ Equal first authorship

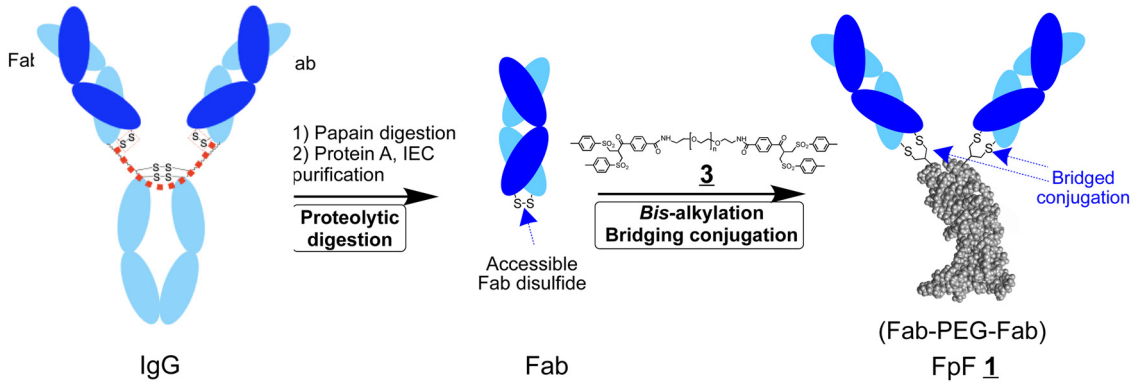

Scheme 1 IgG representation showing how the two Fabs topologically are shown to be at the two ends of a flexible linear molecule (note the red dotted line). Proteolytic digestion of the IgG provides the corresponding Fab after purification which can be conjugated to each end of the di(bis-sulfone) reagent **3** to give FpF **1**.

FpFs are prepared using the di(bis-sulfone) reagent **3** to conjugate 2 Fabs that can be obtained by the proteolytic digestion of IgGs (Scheme 1).[1] Each bis-sulfone conjugation moiety in the di(bis-sulfone) reagent **3** undergoes site specific bis-alkylation conjugation with the two thiols from the accessible Fab disulfide furthest from the target binding region by a sequence of addition–elimination reactions to give thiol ethers that are more stable than the initial disulfide (Scheme S1, ESI†).[7,8] Di(bis-sulfone) **3** has also been used to dimerise other proteins by bis-alkylation of cysteine thiols[9,10] including an analogous Fc-fusion mimetic[10] which involved conjugating the extracellular receptor binding domains of an Fc-fusion protein. The Fc-fusion mimetic is called a RpR for receptor–PEG–receptor and displayed better binding characteristics compared to the corresponding parent Fc-fusion, aflibercept.

Bispecific antibody-based medicines are clinically proven modalities used to treat cancer, heamophilia and neovascular retinal diseases[11–16] with many clinical candidates undergoing development with encouragement from the regulatory authorities. Faricimab is a bispecific antibody that binds to 2 ligands in the vitreous cavity to treat retinal diseases. Intravitreal injections are administered in a small volume (50 μL) and are difficult for patients to endure. Increasing residence time in the vitreous is broadly proportional to the concentration of an antibody-based medicine in the formulation.[17] Utilising a high concentration of a single (bispecific) antibody in an intravitreal injection provides better clinical benefits than multiple intravitreal injections of a combination of antibodies.

Bispecific antibodies can also bring two targets together to cause an enhanced biological function not possible by using a combination of 2 separate antibodies. Such spatial–temporal properties have been shown to bring (i) two cells together (*e.g.* blinatumomab and epcoritamab)[13,14] to enhance immune recognition and (ii) two proteins together that are necessary to maintain the coagulation cascade (*e.g.* emicizumab).[16] BsFpFs utilise PEG linkers of a sufficient molecular weight designed to optimise spatial–temporal relationships.

IgGs are multifunctional molecules that can also exert immune-related effector functions through Fc. Many clinically used mono-specific antibodies exert an effector function which is important for their clinical efficacy. Some Fc effector functions can cause inadvertent immune-driven agonism,[18,19] but IgG_4 subtypes are sometimes used to abrogate unwanted Fc-induced effector functionality.[18] Many applications where the spatial–temporal properties of a bispecific antibody can be exploited do not require Fc effector functions.

The concept of bispecific antibodies has been considered for decades[20] as well as their preparation by chemical conjugation.[21–23] Purely recombinant strategies are used for the preparation of clinically used bispecific antibodies,[24] but challenges remain to optimise the structure and format of bispecific antibodies for researchers in early preclinical research.[24–26] The use of chemical conjugation and modification strategies to aid in the development of therapeutic proteins including antibody-based molecules is widespread, clinically proven and is being driven by much creative research studies.[27–34] There is also intense interest in developing protein–protein and protein–drug conjugates[35–38] as the combined use of recombinant and conjugation technologies may yield complex molecules for study and potential development.

Our goal is to develop a practical method to prepare bsFpFs, making these valuable tools readily accessible to researchers interested in a wide range of preclinical research including drug target development, drug delivery, tissue engineering and immunocytochemistry. We first explored the di(bis-sulfone) reagent **3** to prepare bispecific FpFs **2** (Scheme 2) in a conjugation-only approach. Since the preparation of bsFpFs with the di(bis-sulfone) reagent **3** requires the sequential addition of 2 different Fabs, there can be limitations due to the formation of small amounts of homodimeric FpF during the addition of the first Fab, so we also examined a conjugation–ligation strategy for the preparation of bispecific FpFs (Scheme 6). The conjugation–ligation strategy enabled the synthesis of an extensive panel of seventeen different bsFpFs, targeting a diverse range of therapeutic molecules implicated in ocular inflammation (TNF-α, IL6R, IL17, and VEGF) and ocular drug delivery (hyaluronic acid and collagen II). To the best of our knowledge, this represents the first synthesis of such a

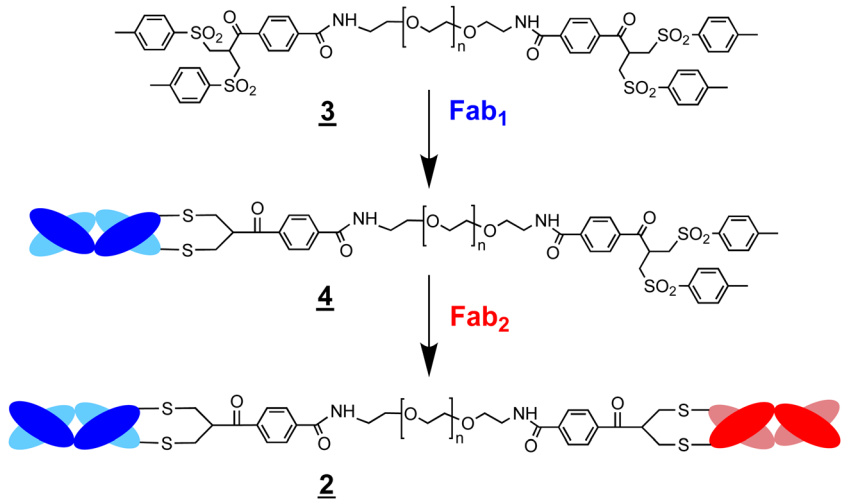

Scheme 2 Preparation of a bsFpF **2** by the conjugation of Fab_1 with an excess di(bis-sulfone) reagent **3**. The intermediate conjugate **4** can be purified by IEX and in some cases by spin filtration to remove the excess starting reagent **3** and unreacted Fab_1. Conjugation of Fab_2 to the intermediate conjugate **4** gives the bsFpF **2**.

broad spectrum of bsFpFs which would be more costly and difficult to achieve by recombinant means alone.

Experimental section

Materials

Bevacizumab (Avastin®, 25 mg mL^{-1}, anti-VEGF IgG), infliximab (Remicade®, 10 mg mL^{-1}, anti-TNFα IgG), tocilizumab (Avtemra®, 20 mg mL^{-1}, anti-IL6R IgG) and ranibizumab (Lucentis®, 10 mg mL^{-1}, anti-VEGF Fab) were obtained from the pooled remaining contents of vials that had been used clinically. Secukinumab (Cosentyx®, 150 mg) was purchased commercially. Phosphate buffered saline (PBS; 0.16 M NaCl, 0.003 M KCl, 0.008 M Na2HPO4 and 0.001 M KH2PO4) was prepared with tablets purchased from Oxoid. Acetate buffer A (100 mM sodium acetate, pH 4.0) and acetate buffer B (100 mM sodium acetate, 1 M NaCl, pH 4.0) were prepared for ion-exchange chromatography. Novex bis–tris 4–12% gels, sharp blue standard protein markers, NuPAGE MOPS running buffer, NuPAGE LDS sample buffer and SilverXpress silver staining kit were purchased from Invitrogen. InstantBlue was purchased from Expedeon Ltd. Perchloric acid (0.1 M) and barium chloride (5.0%) solutions for barium iodide staining were prepared in the lab. A PD-10 column, cation exchange columns (HiTrap SP HP 1.0 mL) and a Superdex 200 prep grade size exclusion column (34.0 μm particle size) along with Biacore consumables were all purchased from GE Healthcare. Anti-human IgG (Fab specific)-peroxidase, 3,3′,5,5′-tetramethylbenzidine (TMB) and human vascular endothelial growth factor ($hVEGF_{165}$) were purchased from Sigma Aldrich.

Methods

Fab isolation. Proteolytic digestion of bevacizumab, infliximab, tocilizumab and secukinumab was performed. The digestion method for digesting these IgGs has been optimised previously in our lab.[39] In brief, a pre-digestion buffer (200 mL, 20 mM NaH_2PO_4, 10 mM EDTA) with pH 7.0 was prepared. The pH of the solution was checked to ensure that it remained at pH 7.0 ± 0.5 and was adjusted if necessary. An IgG antibody (15 mg, 1 mL) was prepared using a digestion buffer. Lyophilised papain (150 μL at 5 mg mL^{-1}) was then added to prepare a 1 : 20 papain:IgG ratio. The digestion mixture was placed in an incubator at 37 °C for 30 minutes. The crude digestion mixture was then purified using protein L chromatography (Hitrap Protein L) using buffer A (100 mM sodium phosphate, 150 mM sodium chloride, 500 mL, pH 7.2) and buffer B (100 mM glycine, 500 mL, pH 2.5) and an elution gradient.

Eluted fractions were monitored using SDS–PAGE and further purified using an SEC (Superdex 200 Increase 10/300 GL, flow rate of 0.5 mL min^{-1} and PBS as the mobile phase). Eluted fractions were collected and monitored using SDS–PAGE.

Representative bsFpF preparation by the di(bis-sulfone) reagent 3. Fab_{VEGF} (1.0 mg in 1.0 mL of conjugation buffer; 20 mM sodium phosphate, 10 mM EDTA, pH 7.6) was first incubated with DTT (1.0 mg) at ambient temperature without shaking for 30 min. DTT was removed by elution over a PD-10 column. Into 1.0 equivalent of reduced-Fab_{VEGF} was added the di(bis-sulfone) PEG_{10} reagent **3**[1] (5 equivalents, 1 mg) and the solution was incubated for 1 h at ambient temperature. The PEGylation reaction mixture was then purified using a Macrocap SP cation exchange column (Macrocap SP, 5 mL). The IEX-purified bis sulfone–PEG_{10}–Fab_{VEGF} was then incubated with the pre-DTT treated Fab_{HER2} (1.0 mg in 3.3 mL after the PD-10 column). The formation of bispecific Fab_{VEGF}–PEG_{10}–Fab_{HER2} was then monitored for 2, 15 and 48 hours at ambient temperature using SDS–PAGE. The Fab_{VEGF}–PEG_{10}–Fab_{HER2} was purified using single-step size-exclusion chromatography (SEC), and SEC fractions were analysed by SDS–PAGE.

Representative bsFpF preparation by conjugation–ligation. Fab_{VEGF} (1.0 mg in 1.0 mL of conjugation buffer; 20 mM

sodium phosphate, 10 mM EDTA, pH 7.6) was incubated with DTT (1.0 mg) at ambient temperature without shaking for 30 min. DTT was removed by elution over a PD-10 column. Bis-sulfone–PEG–TCO **28** (0.1 mL, 4.0 mg mL^{-1} in distilled water, 1.0 eq.) was then added to the reduced Fab_{VEGF} solution (1.0 mg in 3.3 mL). The PEGylation solution was incubated at ambient temperature for approximately 6 h without shaking. In a separate vial, Fab_{IL6R} (1.0 mg in 1.0 mL of conjugation buffer; 20 mM sodium phosphate, 10 mM EDTA, pH 7.6) was incubated with DTT (1.0 mg) and the DTT was removed by elution over a PD-10 column. Bis-sulfone–PEG–Tz **30** (0.1 mL, 2.0 mg mL^{-1} in distilled water) was then added to the reduced Fab_{IL6R} solution (1.0 mg in 3.3 mL). The PEGylation solution was incubated at ambient temperature for approximately 6 h without shaking. Both PEG–Fab conjugates (Fab_{VEGF}–PEG TCO **29** and Fab_{IL6R}–PEG Tz **31**) were purified using a Macrocap SP cation exchange column (Macrocap SP, 5 mL). Fractions (1.0 mL) were analysed by SDS–PAGE. Purified intermediate molecules **29** and **31** were then mixed for approximately 18 hours at 4 °C to undergo ligation, forming a bsFpF molecule **2**. bsFpFs were then purified using cation exchange chromatography followed by SEC. The purity of the bsFpF was assessed using silver staining and the concentration of the purified bsFpF was calculated using a micro-BCA assay.

The products are denoted using subscript '*n*' on PEG_n to indicate the PEG molar weight, *e.g.* FabVEGF–PEG15–$FabTNF_\alpha$ is derived from the FabVEGF from bevacizumab, $FabTNF_\alpha$ from infliximab, the 10 kDa for the PEG_{10} reagent **28** and the 5 kDa for the PEG5 reagent **30**.

Comparative binding determined by ELISA. A flat bottom 96-well plate was coated with VEGF (100 μL of a 1 μg mL^{-1} VEGF solution, 0.1 μg VEGF per well) and incubated overnight at 4 °C. The next day, the VEGF solutions were removed and without washing, blocking buffer (300 μL, PBS with 1% BSA and 0.05% Tween 20) was added into each well and incubated at ambient temperature for 2.0 h. After this, the blocking buffer was aspirated and the plate was washed once with washing buffer (300 μL, PBS with 0.05% Tween 20) and then tested compounds, which were prepared in PBS at a range of concentrations, were added into each well (100 μL). The plate was incubated for 2.0 hours at ambient temperature. After 2.0 h incubation, the protein solutions were removed and wells were washed with washing buffer (300 μL) three times. Then, anti-human Fab_2 (Fab specific)-peroxidase (100 μL, 1/5000 dilution) was added into each well and incubated for 1.0 hours at ambient temperature. The solutions were then removed, and the plate was washed off with a washing buffer three times. TMB (100 μL) was then added, and the development of the blue colour was monitored. After approximately 5 min, when the blue colour was visible enough for each well, HCl (50 μL, 1.0 M) solution was added to produce a constant yellow colour. The plate was then read using a plate reader at 450 nm wavelength. The data were processed using a graph pad prism (V9) and affinities were generated using one site-specific binding fitting method. No adjustments to the methodology were made for IL-6R, and ligand concentrations, incubation times and washing steps were identical.

Comparative binding determined by SPR (Biacore). For binding molecules, human recombinant $VEGF_{165}$ (38 kDa) was immobilised on a CM3 chip at an immobilisation level of 95 RU using standard carbodiimide-mediated coupling (NHS/EDC, 50/50) and ethanolamine (pH 8.5). Samples were prepared in HBS-EP running buffer (10 mM HEPES, pH 7.4, 150 mm NaCl, 3.0 mM EDTA, 0.005% surfactant P20). All kinetic measurements were conducted at 25 °C at a flow rate of 30 μL min^{-1} with an association time of 180 s and dissociation rate of 1200 s. Chip regeneration was accomplished by exposure to 10.0 mM glycine–HCl (pH 2.0) for 1200 s. Double-referencing was performed to account for bulk effects caused by changes in the buffer composition or nonspecific binding. For IL-6R binding molecules, human his-tagged recombinant IL-6R (42 kDa) was captured onto a NTA chip by first activating the chip surface with a nickel (Ni^{2+}) solution. Samples were prepared in HBS-EP running buffer (10 mM HEPES, pH 7.4, 150 mm NaCl, 3.0 mM EDTA, 0.005% surfactant P20). For a TNFα binding molecule, human his-tagged recombinant TNFα was captured onto a NTA chip using a similar procedure described for his-tag IL6R. All kinetic measurements were conducted at 25 °C at a flow rate of 30 μL min^{-1} with an association time of 120 s and a dissociation rate of 1200 s. The NTA chip surface was regenerated with EDTA solution in between each analysis cycle. Data were evaluated with the BIAevaluation software (version 2.1) and the best fit (lowest Chi^2) was obtained using a 1 : 1 binding model. The sensorgram was fitted globally over the association and dissociation phases. Equilibrium dissociation constants (affinity) were calculated from the rate constants ($K_D = k_{off}/k_{on}$).

Microscale thermophoresis of antibodies and antibody conjugates. Antibodies and bispecific antibody mimetics were labelled as per the instructions found in the monolith amine reactive protein labelling kit. An MST assay buffer (50 mM Tris, 150 mM NaCl, 10 mM $MgCl_2$, pH 7.4, and 0.05% w/v Tween 20) was used to dilute the labelled antibody or bispecific antibody mimetic (bsFpF) to a concentration of 5 nM. Serial dilutions of relevant ligands (VEGF, IL6R, 1.0×10^{-6} to 1.52×10^{-11} M) and combined ligands (VEGF + IL6R) were mixed with the labelled antibodies or antibody bsFpF in glass capillaries for measurements. Assays were performed using a LED power of 15% and with a laser power set to high. A Monolith Pico system was used for all MST measurements.

Results

bsFpFs prepared by conjugation

The di(bis-sulfone) reagent **3** derived from PEG with a molecular weight of 10 kDa was used to prepare a bsFpF from Fabs targeted to VEGF and HER2 (Scheme 2). Fabs can be obtained by thiol protease digestion of IgGs using either immobilised or soluble papain.[39] Bevacizumab was the IgG that was proteolytically digested to give the Fab targeted to VEGF and

trastuzumab was the IgG source for the Fab targeted to HER2. The accessible disulfide of Fab_{VEGF} was reduced with dithiothreitol (DTT) (Fig. 1A, lanes 2 and 3).

Fig. 1 After removal of DTT using a PD-10 column,[1,7] the reduced Fab (1.0 mg in 3.3 mL) was allowed to incubate with an excess of the di(bis-sulfone) reagent **3** (5 equivalents, 1 mg) in the PEGylation buffer with pH 7.8 for 1 hour at ambient temperature (Fig. 1A, lane 4). The reaction solution essentially comprised a mixture of the desired intermediate conjugate Fab_{VEGF}–PEG_{10}–bis-sulfone **4**, unreacted di(bis)-sulfone reagent **3**, trace starting Fab_{VEGF} and the undesired homodimer FpF, Fab_{VEGF}–PEG_{10}–Fab_{VEGF}. The excess di(bis-sulfone) reagent **3** was used to minimise the formation of the homodimer, Fab_{VEGF}–PEG_{10}–Fab_{VEGF} (Fig. 1A, lane 4). The reaction mixture was then eluted over an ion exchange column (a MacroCap SP) to give predominantly a band at 70 kDa, thought to be the desired intermediate conjugate Fab_{VEGF}–PEG_{10}–bis-sulfone **4** (Fig. 1A, lane 5). The excess di(bis-sulfone) reagent **3** was removed from the reaction mixture preferably by ion exchange chromatography or by centrifugal filtration to prevent suppression of bsFpF formation.

In a separate vial, Fab_{HER2} (1.0 mg in 1.0 mL of the PEGylation buffer) was incubated with DTT (1.0 mg), then DTT was removed and reduced-Fab_{HER2} (Fig. 1A, lane 6) was incubated with the intermediate conjugate, Fab_{VEGF}–PEG_{10}–bis-sulfone **4** for 12 hours to give the desired bsFpF **2** (Fab_{VEGF}–PEG_{10}–Fab_{HER2}). Scouting reactions (Fig. 1B) indicated that the conjugation of Fab_{HER2} to the intermediate Fab_{VEGF}–PEG_{10}–bis-sulfone **4** required a longer incubation time than conjugation of the first Fab (Fab_{VEGF}) to the starting di(bis-sulfone) reagent **3**.

Purification of the di(bis-sulfone) reagent **3** by HPLC (Fig. S1, ESI†) resulted in better conversion to the desired Fab_{VEGF}–PEG_{10}–Fab_{HER2} **2** (Fig. 1A, lanes 7 and 8) which was purified by size exclusion chromatography (SEC) (Fig. 1A, lanes 9–13). The purity of the bsFpF **2**, Fab_{VEGF}–PEG_{10}–Fab_{HER2}, was confirmed by silver staining (Fig. 1A, lane 14).

Binding of Fab_{VEGF}–PEG_{10}–Fab_{HER2} **2** was evaluated by surface plasmon resonance (SPR) with each ligand immobilised on separate CM3 chips at low response units to allow kinetic studies to be conducted (VEGF (55 RU) and HER2 (65 RU)). Ligand binding was first confirmed with the parent antibodies and bevacizumab for VEGF and trastuzumab for HER2. Additionally, there was no non-specific binding observed when bevacizumab was incubated with the immobilised HER2 chip and when trastuzumab was incubated with the immobilised VEGF chip (Fig. S2A and B, ESI†). The bsFpF **2**, Fab_{VEGF}–PEG_{10}–Fab_{HER2}, displayed concentration-dependent binding to each

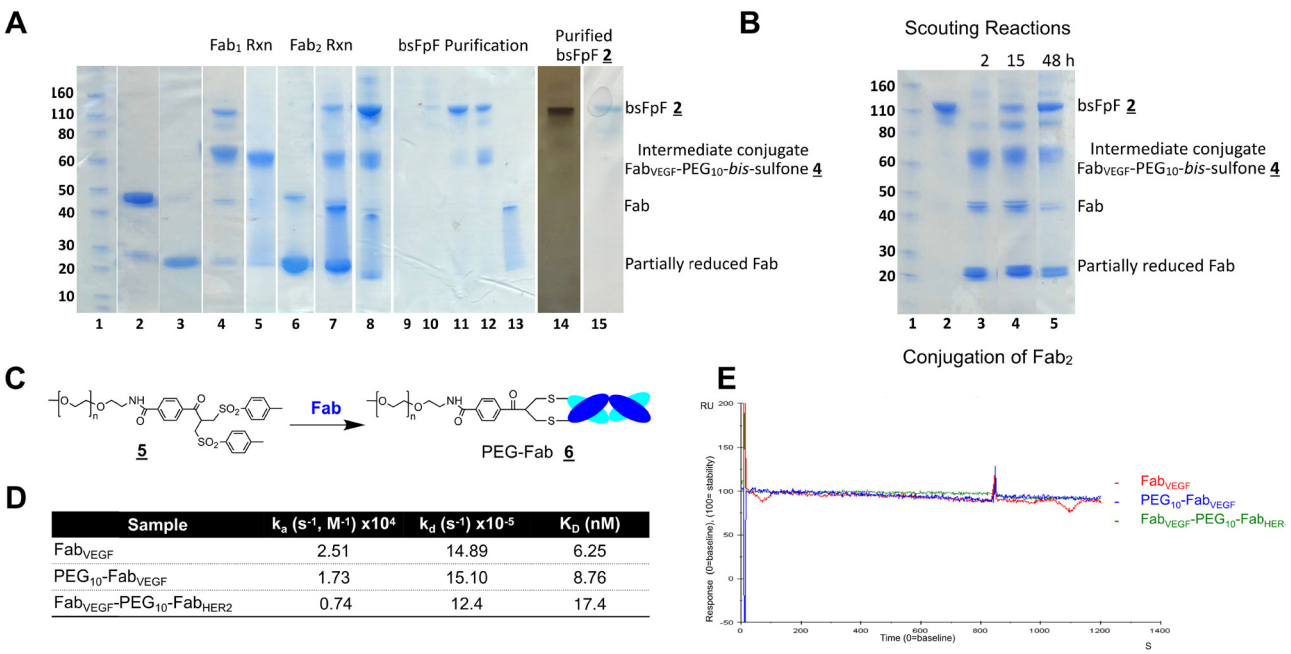

Sample	k_a (s^{-1}, M^{-1}) x10^4	k_d (s^{-1}) x10^{-5}	K_D (nM)
Fab_{VEGF}	2.51	14.89	6.25
PEG_{10}-Fab_{VEGF}	1.73	15.10	8.76
Fab_{VEGF}-PEG_{10}-Fab_{HER2}	0.74	12.4	17.4

Fig. 1 (A) Representative SDS–PAGE analysis for preparation of bsFpF **2** using the di(bis-sulfone) reagent **3** and the SDS-PAGE was stained with instant blue for protein staining (lanes 1–15) and silver staining for detecting any trace of impurity (lane 14), lane 1: Novex pre-stained protein marker, lane 2: Fab_{VEGF} (no DTT), lane 3: Fab_{VEGF} + DTT, lane 4: reaction mixture between PEG reagent **3** (4–5 eq.) and reduced-Fab_{VEGF} (1 eq.) after 1 h incubation at ambient temperature, lane 5: Fab_{VEGF}–PEG–bis sulfone **4** was obtained using ion-exchange chromatography, lane 6: Fab_{HER-2} + DTT, lane 7: reaction mixture between Fab_{VEGF}–PEG–bis sulfone **4** and reduced Fab_{HER-2} (crude PEG reagent **3** was used for first conjugation), lane 8: reaction mixture between PEG–Fab_{VEGF} **6** and reduced Fab_{HER-2} (HPLC purified PEG reagent **3** was used for the conjugation), lanes 9–13, purification fraction using size-exclusion chromatography, lane 14: purified Fab_{VEGF}–PEG_{10}–Fab_{HER-2} **2** and lane 15: purified Fab_{VEGF}–PEG_{10}–Fab_{TNFa} **2** appeared at the 110 kDa MW band. (B) SDS–PAGE analysis for scouting reactions at 2, 15 and 48 h for the conjugation of the second Fab (Fab_{HER2}) to the intermediate conjugate **4** (Fab_{VEGF}–PEG–bis sulfone). (C) Synthesis of PEG–Fab **6**. (D) Average kinetic rate constants and parameters achieved for Fab_{VEGF}, PEG_{10}–Fab_{VEGF} **6** and bispecific Fab_{VEGF}–PEG_{10}–Fab_{HER-2} **2** using a CM3 chip immobilised with VEGF (55 RU). The numbers of replicates were 2 for bispecific conjugate and 3 for other samples. (E) Dissociation profiles overlayed for Fab_{VEGF}, PEG_{10}–Fab_{VEGF} **6** and Fab_{VEGF}–PEG_{10}–Fab_{HER-2} **2**.

immobilised ligand (Fig. S2C and D, ESI†). Both VEGF and HER2 were immobilised to a single CM3 chip and binding of bevacizumab and trastuzumab was observed (control) as well as the concentration-dependent binding of bsFpF, Fab_{VEGF}–PEG_{20}–Fab_{HER2} (Fig. S2E and F, ESI†).

SPR kinetic studies were performed with Fab_{VEGF}, PEG_{10}–Fab_{VEGF} **6** and the bsFpF **2**, Fab_{VEGF}–PEG_{10}–Fab_{HER2} using VEGF immobilised to a CM3 chip. PEG_{10}–Fab_{VEGF} **6** was prepared from the PEG_{10} bis-sulfone reagent **5** used for protein PEGylation as previously described (Fig. 1C).[1,2,40] The SPR data indicated that Fab_{VEGF} exhibited a faster association rate constant (k_a) compared to both PEG_{10}–Fab_{VEGF} **6** and Fab_{VEGF}–PEG_{10}–Fab_{HER2} **2**. This is likely attributed to the smaller molecular weight of Fab_{VEGF}. However, no discernible difference was observed in the dissociation rate constant (k_d) between Fab_{VEGF}, PEG_{10}–Fab_{VEGF} **6** and Fab_{VEGF}–PEG_{10}–Fab_{HER2} **2** upon dissociation from immobilised VEGF (Fig. 1D and E).

A second bsFpF **2** (Fab_{VEGF}–PEG_{10}–$FabTNF_{\alpha}$) derived from Fab_{VEGF} and a Fab targeted to tumour necrosis factor alpha (TNF-α) was prepared using the di(bis-sulfone) reagent **3** (Fig. 1A, lane 15). Fab_{VEGF}–PEG_{10}–$FabTNF_{\alpha}$ also displayed concentration-dependent binding as observed by SPR to both VEGF and TNF-α (Fig. S3, ESI†).

During the preparation of bsFpFs **2** using the di(bis-sulfone) reagent **3**, it was thought that a reagent with more different conjugation reactivity at each PEG terminus would allow more efficient preparation of a bsFpF **2** by a conjugation only approach. It was thought that a reagent with reduced conjugation reactivity on one terminus would require a lower excess of the FpF reagent for the first Fab conjugation while producing a less homodimer.

The bis-sulfone conjugation moiety functions by a sequence of addition–elimination reactions (Scheme S1, ESI†). Initial elimination of one equivalent of the toluene sulfinic acid leaving group **8** is necessary to generate the α,β-unsaturated carbonyl moiety (*e.g.* structure **9**, Scheme 3A). The initial elimination reaction is driven by the pK_a of the α-proton to the carbonyl electron-withdrawing group in the bis-sulfone conjugating moiety **7** (Scheme 3A). If the pK_a value of the α-proton was increased slightly as in the bis-sulfide precursor **10** (Scheme 3A), this would reduce the rate of the initial elimination step to potentially slow conjugation compared to the bis-sulfone moiety.

The conjugation reactivity of the bis-sulfone moiety **7** is also due to the pK_a of the toluene sulfinic acid leaving group **8** (Scheme 3B) which we estimate to be about ~1.6 and is much lower than that for the cysteine thiol (pK_a ~ 10) to drive conjugation. Increasing the pK_a of the leaving groups (*e.g.* structures **11** and **13**–**15**, Scheme 3) relative to toluene sulfinic acid **8** would potentially contribute to reduced conjugation reactivity. We therefore sought to examine the asymmetric conjugation reagent **16** (Scheme 4). A bsFpF could potentially be made by conjugation to the bis-sulfone moiety with the first Fab (Fab_1) and then conjugation of the second Fab (Fab_2) to the

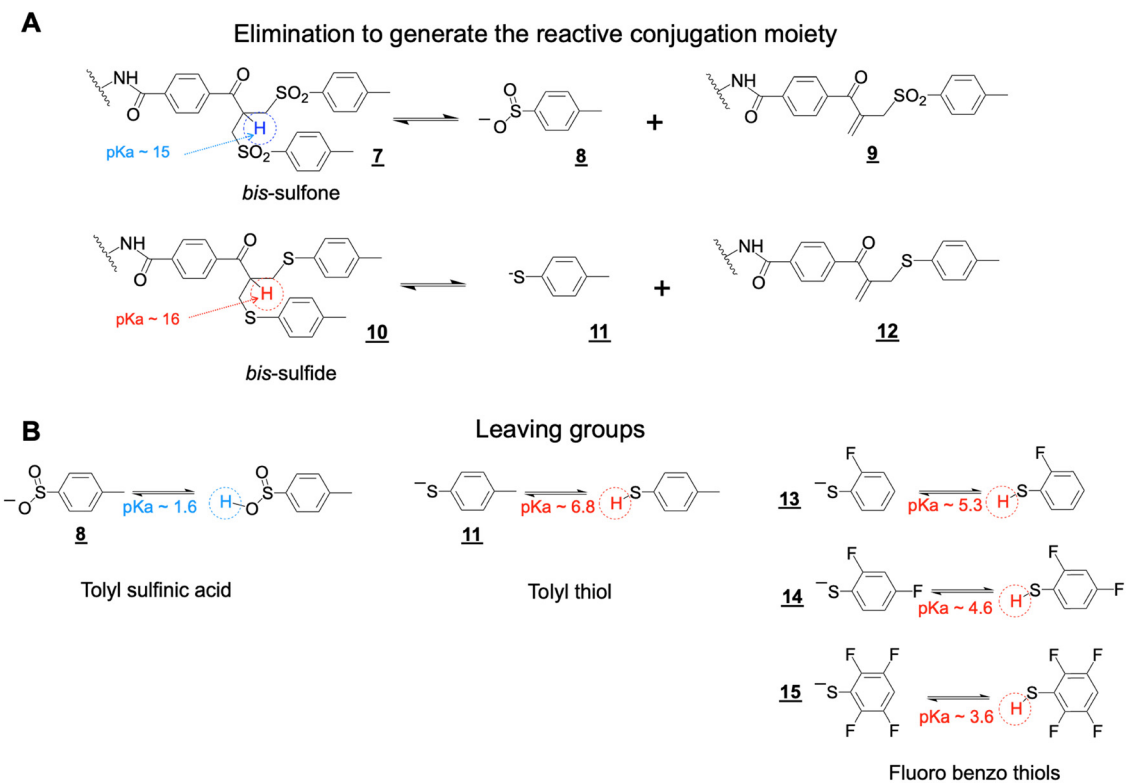

Scheme 3 (A) Elimination reactions of the bis-sulfone **7** and bis-sulfide **10** conjugation moieties to yield enones capable of alkylation by a thiolate from a reduced disulfide. The pK_a value of the α-proton in bis-sulfone **7** is thought to be slightly less than that of the α-proton in bis-sulfide **10**. (B) Estimates of leaving group pK_as.

less reactive bis-sulfide moiety in the intermediate Fab–PEG–bis sulfide intermediate **17** (Scheme 4).

We prepared the bis-sulfide PEGylation reagents **18**, **19**, **20**, and **21** (Structures 2) to examine relative conjugation reactivities with the PEG–bis sulfone **5** (Fig. 1C). PEG_{10}–bis-sulfide **18** with the unsubstituted tolyl thiol leaving group was not reactive enough under the mild conditions normally employed for Fab conjugation (Figures S4A and B, ESI†). In contrast, the aryl tetra-fluoro thiol leaving group in PEG_{10}–bis sulfide **21** appeared to have comparable conjugation reactivity with the bis-sulfone moiety in PEG–bis sulfone **5** (Figure S4A, ESI†).

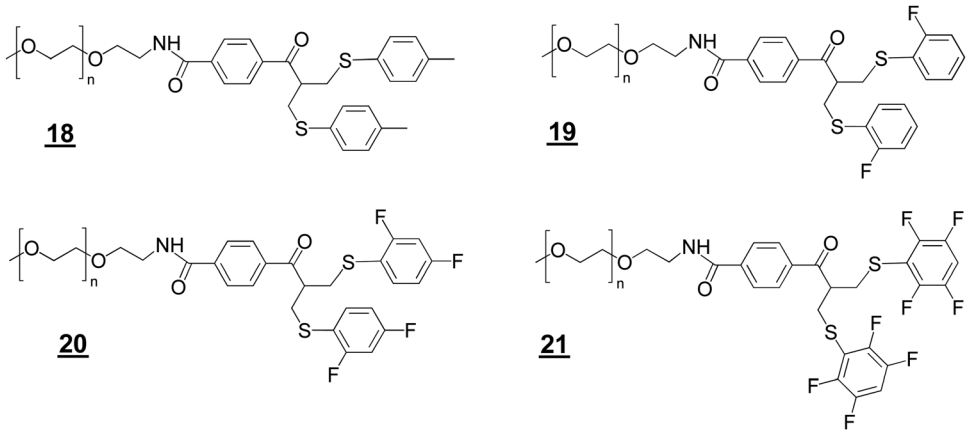

The *ortho*-fluoro and di-fluoro PEG_{10}–bis sulfides **19** and **20** underwent Fab conjugation (Fig. 2A and B). Reagents **19** and **20** appeared to have sufficient conjugation reactivity while being less reactive than that of the bis-sulfone moiety. An experiment to examine the sequential conjugation reactions of Fab_{VEGF} to *ortho*-fluoro bis-sulfide bis-sulfone reagent **22** did appear to give a good conversion to homodimeric FpF **1** (Fig. 2C). An analogous conjugation was conducted with the di-fluoro bis-sulfide bis-sulfone reagent **23** where formation to the desired FpF (Fig. S4C, ESI†) was also observed. These preliminary efforts indicated that considerable Fab_2 remained which made the IEX purification difficult necessitating SEC purification. Fab_2 conjugation also appeared to be slower with the intermediate conjugate Fab_1–PEG–bis sulfide intermediate **17** than Fab conjugation with PEG–fluoro-bis-sulfone (*e.g.* **19**).

bsFpFs prepared by conjugation–ligation

Considering the encouraging binding properties of Fab_{VEGF}–PEG_{10}–Fab_{HER2}, we wanted to evaluate a larger number of bsFpF molecules. The di(bis-sulfone) **3** and the asymmetric conjugation bis-sulfide bis-sulfone reagents **16** are good reagents and can be used to prepare a bsFpF or other heterodimeric protein conjugates. To prepare several bsFpFs that could be used in early preclinical research, we decided to examine preparing these molecules by a conjugation–ligation strategy (Scheme 5). Conjugation–ligation strategies to prepare protein–protein and protein–drug conjugates are well

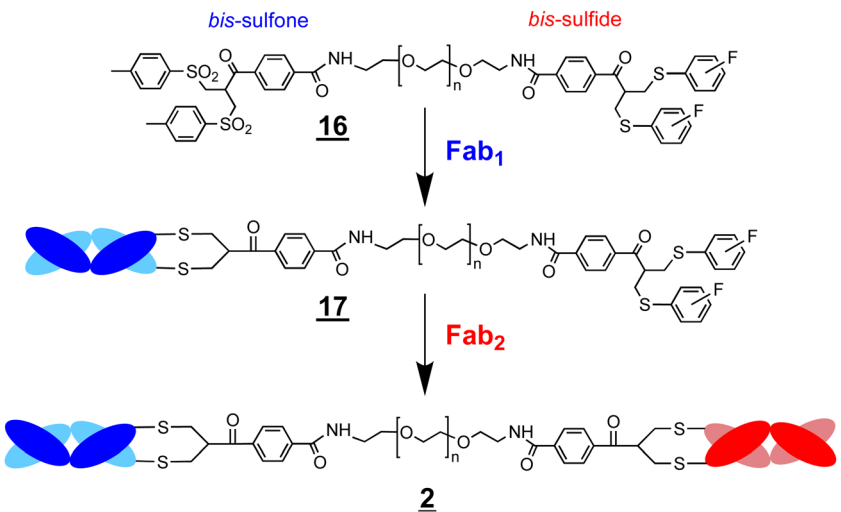

Scheme 4 Preparation of a bsFpF **2** by the conjugation of Fab_1 with the bis-sulfone bis-sulfide reagent **16**. Conjugation is intended to occur on the bis-sulfone moiety of reagent 16 to give the intermediate conjugate **17** can be purified by IEX or by spin filtration to remove the excess starting reagent **16** and unreacted Fab_1. Conjugation of Fab_2 to the intermediate conjugate **17** gives the bsFpF **2**.

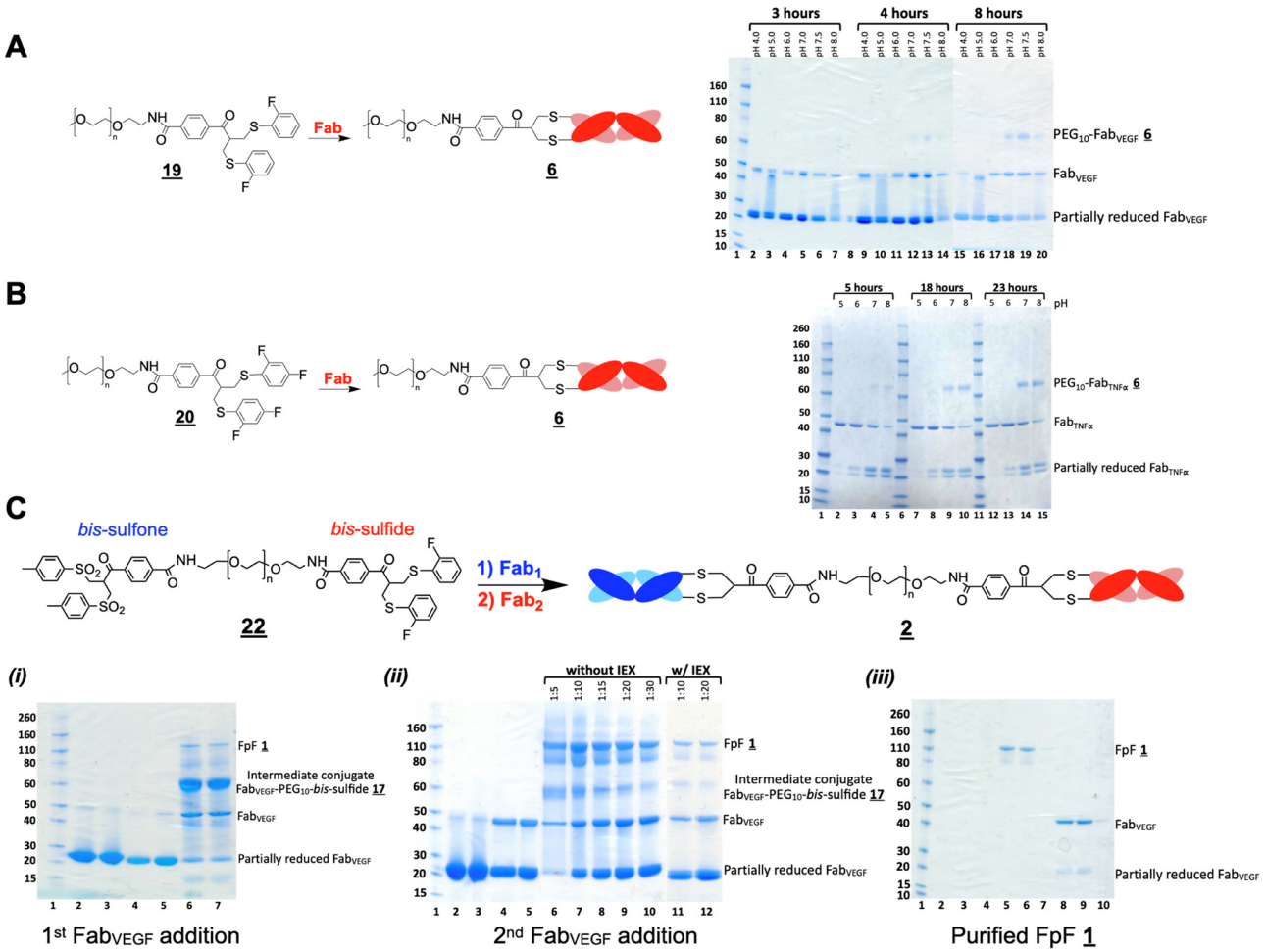

Fig. 2 Conjugation of fluorodisulfide reagents (novex BisTris 4–12% gel stained with oomassie blue). (A) Scouting conjugation of Fab_{VEGF} to PEG_{10}–bis-sulfide *ortho*-fluoride **19** (2 eq.) from pH 4 to 8 at different incubation times. Lane 1: protein markers, lanes 2–7: 3-hour incubation time, lane 8: blank, lanes 9–14: 18-hour incubation time, lanes 15–20: 23-hour incubation time. (B) Scouting conjugation of $Fab_{TNF\alpha}$ to PEG_{10}–bis-sulfide-difluoride **20** (2 eq.) from pH 5 to 8 at different incubation times. Lane 1: protein markers, lanes 2–5: 5-hour incubation time, lane 6: protein markers, lanes 7–10: 18-hour incubation time, lane 11: protein markers, lanes 12–15: 23-hour incubation time. (C) Scouting reactions to prepare a FpF in two steps using the *ortho*-fluoro bis-sulfide bis-sulfone reagent **22**. The same Fab_{VEGF} was used in both conjugation steps, so FpF **1** was prepared rather than a bsFpF **2**: (i) first Fab_{VEGF} conjugation reaction, lane 1: protein markers, lanes 2–3: 2 batches of reduced Fab_{VEGF} before PD10 elution, lanes 4 and 5: reduced Fab_{VEGF} after PD10 elution, lanes 6 and 7: first conjugation of Fab_{VEGF} to the reagent **22**. (ii) Second Fab_{VEGF} conjugation reaction, lanes 2 and 3: 2 batches of reduced Fab_{VEGF} before PD10 elution, lanes 4 and 5: reduced Fab_{VEGF} after PD10 elution, lanes 6–10: second conjugation of increasing stoichiometries of Fab_{VEGF} with the corresponding intermediate conjugate, Fab_{VEGF}–PEG_{10}–*ortho* bis sulfone **17**, which had not been eluted over an IEX column, lanes 11 and 12: second conjugation of increasing stoichiometries of Fab_{VEGF} with the corresponding intermediate conjugate, Fab_{VEGF}–PEG_{10}–*ortho* bis sulfone **17**, which had been eluted over an IEX column. (iii) Fractions from SEC purification of the FpF **1**, Fab_{VEGF}–PEG_{10}–Fab_{VEGF} after a first step of IEX elution.

known.[41–43] In principle, conjugation ligation reagents **24** and **25** are first used to site-specifically modify separate proteins by disulfide rebridging conjugation to give intermediate conjugates **26** and **27** that can be ligated to give the desired bsFpF **2**. Different Fabs can be used to provide stock solutions of the intermediate conjugates **26** and **27** that can be ligated to form a family of bsFpFs. Such an approach minimises the number of protein conjugation reactions needed and the need to purify bsFpFs from the unmodified protein.

The ligation step requires reactive moieties that will not undergo a reaction with the conjugated protein. Many ligation strategies and chemical moieties have been described, and we focus here on ligation moieties capable of undergoing cycloaddition.[41,43] To prepare bsFpFs by a conjugation–ligation approach, we examined the bis-sulfone *trans*-cyclooctene (TCO) and tetrazine (Tz) reagents **28** and **30** (Scheme 6). The bis-sulfone–PEG–TCO reagent **28** was derived from a mono-Boc protected PEG di-amine precursor with a molecular weight of either 5 and 10 kDa and the bis-sulfone–PEG–Tz reagent **30** was derived from a PEG precursor of 5 and 10 kDa (ESI†). The TCO and Tz bis-sulfone reagents **28** and **30** readily underwent ligation at pH values ranging from 5 to 9 (ESI,† Fig. S5). Several Fabs were conjugated to the TCO and Tz bis-sulfone reagents **28** and **30** using our standard conjugation conditions with 1.5 to 2.0 equivalents of the conjugation reagent[40,44] to produce intermediate Fab conjugates **29** and **31** for ligation (Scheme 6).

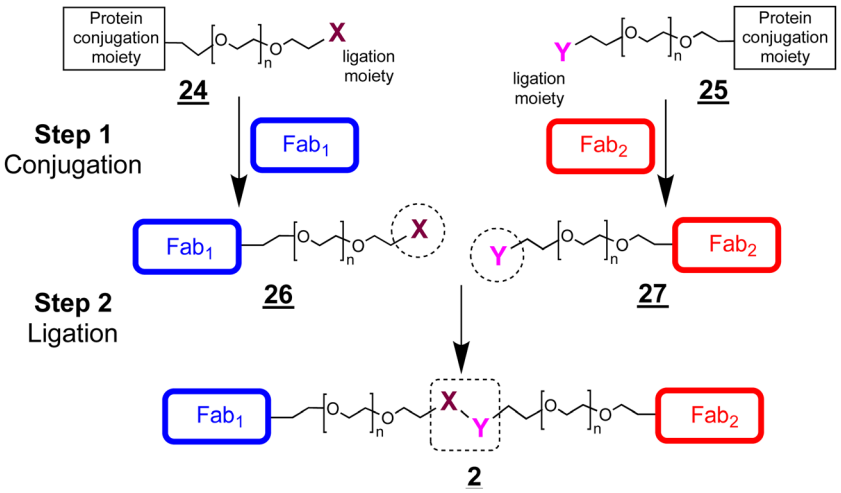

Scheme 5 A conjugation–ligation strategy to prepare bsFpFs **2**. The conjugate intermediates (*e.g.* **26** and **27**) can be used with different Fabs in different combinations to prepare families of bsFpFs **2**.

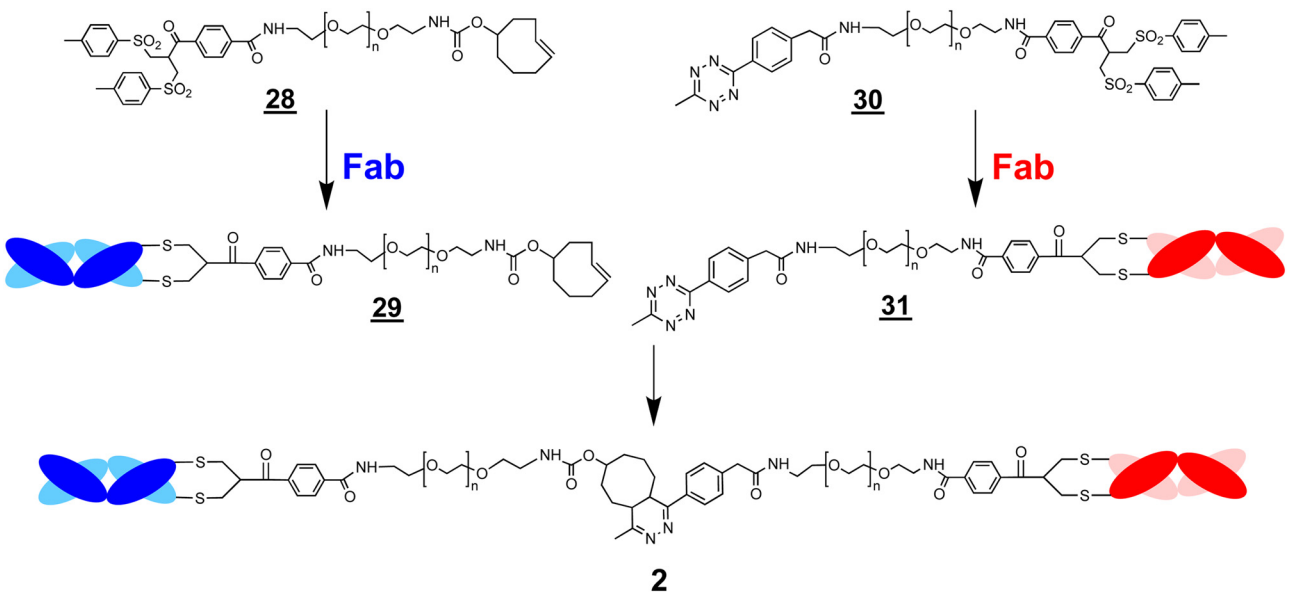

Scheme 6 A conjugation–ligation strategy using the reagents, bis-sulfone–PEG–TCO **28** and bis-sulfone–PEG–Tz **30**, to prepare bsFpFs **2**. The PEG–Fab conjugate intermediates **29** and **31** are prepared by site-specific conjugation of two different Fabs through the bis-sulfone functional group. Ligation of these conjugate intermediates results in the preparation of the bsFpF **2**.

A representative SDS–PAGE gel is shown in Fig. 3 displaying the intermediate conjugates **29** and **31** (lanes 4 and 5). Ligation to produce the bsFpF **2** (or the homodimeric FpF **1**) was accomplished by first eluting the individual conjugation reaction mixtures over an ion exchange column to remove any unconjugated TCO and TZ bis-sulfone reagents **28** and **30**. It was also possible to remove unconjugated reagents by viva spin. A representative ligation reaction mixture is shown in the gel in Fig. 3 (lane 6). Purification of the final bsFpFs **2** was achieved by IEX and SEC with examples shown in lanes 7 to 12 (silver staining was used for detection in lanes 9–12) with the bsFpFs displaying a band at about 115 kDa (Fig. 3).

Fig. 3 Several clinically approved IgGs including bevacizumab (for anti-VEGF Fab), tocilizumab (for anti-IL6R Fab), infliximab (for anti-TNFα Fab) and secukinumab (for anti-IL17 Fab) were digested to provide the Fabs that were used. We have previously described scaling of the papain digestion process to accommodate 100 mg of IgG resulting in the isolation of 50 mg of pure and stable Fab.[39] Table 1 lists the bsFpFs that were prepared by conjugation–ligation using the TCO and Tz bis-sulfone reagents **28** and **30**. To facilitate binding comparisons, the homodimer FpF_{VEGF} was also prepared using the same reagents **28** and **30**, with Fab_{VEGF} sourced from digestion of bevacizumab. Additionally, another homodimer FpF_{VEGF}

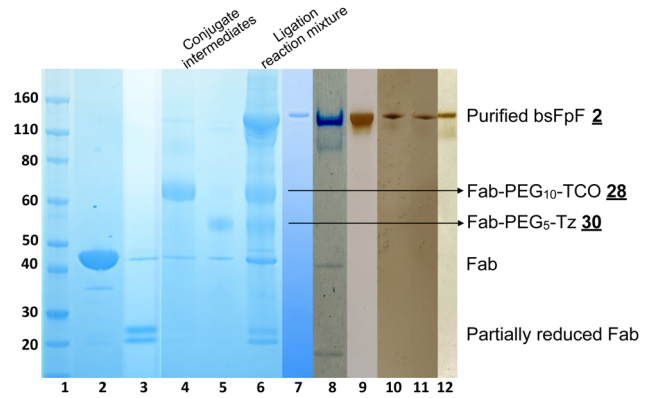

Fig. 3 Representative SDS–PAGE analysis for preparation of bsFpF **2** using the bis-sulfone conjugation–ligation reagents **28** and **30**, and the SDS–PAGE was stained with instant blue for protein staining (lanes 1–8) and silver staining for detecting any trace of impurity (lanes 9 to 12), lane 1: protein markers, lane 2: Fab_{VEGF}, lane 3: reduced Fab_{VEGF}, lane 4: Fab_{VEGF} conjugated to the bis-sulfone–PEG_{10}–TCO reagent **28**, lane 5: Fab_{VEGF} conjugated to the bis-sulfone–PEG_5–Tz reagent **30**, lane 6: reaction mixture for the ligation reaction between conjugate intermediates Fab_{VEGF}–PEG_{10}–TCO **28** and Fab_{VEGF}–PEG_5–Tz **30**, lanes 7–12: purified bsFpFs **2** (Fab_1–PEG_{15}–Fab_2, silver stain used for lanes 9–12 to assess purity). Different Fabs are used for conjugation; lane 7: homodimer Fab_{VEGF}–PEG_{15}–Fab_{VEGF}, lane 8: Fab_{VEGF}–PEG_{15}–Fab_{HA}, lane 9: Fab_{VEGF}–PEG_{15}–Fab_{IL6R}, lane 10: Fab_{VEGF}–PEG_{15}–$FabTNF_{\alpha}$, lane 11: Fab_{IL6R}–PEG_{15}–$FabTNF_{\alpha}$, and lane 12: Fab_{VEGF}–PEG_{15}–Fab_{COL2}.

Table 1 List of all the bsFpFs, prepared using conjugation–ligation reagents **32** and **34** targeting pro-inflammatory targets (TNFα, IL6R and IL17) and pro-angiogenic target (VEGF) and affinity targets (HA and collagen-2) along with their isolation yields

Fab_1	Fab_2	bsFpF **2** Isolated yields %
Fab_{VEGF}	Fab_{IL6R}	20
Fab_{VEGF}	$Fab_{TNF\alpha}$	16
$Fab_{TNF\alpha}$	Fab_{IL6R}	14
Fab_{VEGF}	Fab_{IL17A}	11
$Fab_{TNF\alpha}$	Fab_{IL17A}	11
Fab_{VEGF}	Fab_{COL2}	13
Fab_{VEGF}	Fab_{HA}	12

construct was prepared using the di(bis-sulfone) reagent **3**. The concentration of both FpFs **1** and bsFpFs **2** was determined by the micro-BCA-assay. Isolated yields varied between 15 and 20% at the reaction scales used and typically about 0.2 mg of purified bsFpF could be obtained starting from 1 mg of each Fab.

A conjugation–ligation–conjugation strategy was also examined (Scheme 7). The Fab_{VEGF}–PEG_{10}–TCO conjugate **29** was ligated with the Tz–PEG_5–bis-sulfone reagent **30** (1.5 equivalents) to give the ligation intermediate, Fab_{VEGF}–PEG_{15}–bis-sulfone **32** (Fig. 4, lane 6). The Fab targeted to an interleukin-6 receptor (Fab_{IL6R}) was then conjugated to intermediate **32** to give the final bsFpF **2** (Fab_{VEGF}–PEG_{15}–Fab_{IL6R}) (Fig. 4, lane 7). The conversion to give this bsFpF, Fab_{VEGF}–PEG_{15}–Fab_{ILR6} appeared to be about the same as when prepared by ligation of the separate conjugate intermediates **29** and **31** (Scheme 6).

We also prepared bis-sulfone–PEG_3-N_3 **33** and bis-sulfone–PEG_5–DBCO **35** (ESI,† Fig. S6) to examine the well-known strain-promoted alkyne–azide cycloaddition which uses azide (N_3) and dibenzocyclooctyene (DBCO) moieties for ligation.[42,45,46] Good conjugation conversion with $Fab_{TNF\alpha}$ was achieved with 1.5 to 2.0 equivalents of the bis-sulfone reagents **33** and **35** after a 5-hour incubation time at pH 8 to give the respective conjugate intermediates **34** and **36** (ESI,† Fig. S6A and B). The conjugation solutions were centrifuged using a viva spin column to remove excess starting reagents. Upon mixing the intermediate conjugates **34** and **36** (ESI,† Fig. S6C), the desired homodimeric FpF **1** was formed but at apparently lower conversion than with the corresponding conjugate intermediates derived from the TCO and Tz bis-sulfone reagents **28** and **30**. Similar ligation results were observed for preparation of the homodimeric FpF derived from Fab_{VEGF} (ESI,† Fig. S7A) and ligation could not be improved when an excess reagent was removed by IEX chromatography instead of viva spin. Commercially available methoxy PEG_{10}–DBCO and bis-sulfone PEG_3-N_3 did undergo ligation as would be expected without the presence of the conjugated Fabs (ESI,† Fig. S7B, lane 4).

The presence of the conjugated protein in each ligation intermediate (*e.g.* Fab–PEG-N_3 **34** and Fab–PEG–DBCO **36**, ESI,† Fig. S6) may have resulted in conformational masking of the hydrophobic ligation moiety in the relatively large PEG linker element when one terminus of the PEG is conjugated to a 50 kDa protein (*i.e.* Fab). The TCO and Tz moieties are known to undergo faster ligation than the azide and DBCO moieties[43] and this may allow more efficient ligation of the Fab conjugate intermediates. Shorter PEG linkers would be expected to allow more facile ligation.

The ELISA was first used to evaluate the binding affinity of Fab_{VEGF}–PEG_{15}–Fab_{IL6R}. Separate plates were coated with VEGF and IL6R. There was no non-specific binding observed when infliximab (anti-TNFα IgG) was incubated with the VEGF or IL6R coated plates. The binding affinities (K_D) determined by the ELISA for the parent anti-IL6R antibody (tocilizumab) and the associated Fab_{IL6R} obtained by proteolytic digestion were 0.13 nM for tocilizumab and 1.50 nM for Fab_{IL6R} (ESI,† Fig. S8). As expected, tocilizumab exhibited a lower K_D and higher binding affinity due to its bivalent nature as an IgG compared to the monovalent Fab_{IL6R}. ELISA affinities represent average values from two replicates. The ELISA binding affinity of the bispecific Fab_{VEGF}–PEG_{15}–Fab_{IL6R} to VEGF (K_D 1.80 nM) and IL6R (K_D 2.55 nM) is shown in Fig. 5. For comparison, the ELISA derived binding of PEG_{10}–Fab_{VEGF} (K_D 2.25 nM) and PEG_5–Fab_{IL6R} (K_D 3.20 nM) was determined (Table 2).

The binding affinity of Fab_{VEGF}–PEG_{15}–Fab_{IL6R} was also evaluated by SPR. $VEGF_{165}$ was immobilised to a CM3 chip (95 RU) and his-Tag IL6R was immobilised to a nitrilotriacetic acid (NTA) chip. The precursor Fabs and PEG–Fab conjugates were used for comparison (*i.e.* Fab_{VEGF}, Fab_{IL6R}, PEG_{10}–Fab_{VEGF} and PEG_5–Fab_{IL6R}). The concentration-dependent binding of the bispecific Fab_{VEGF}–PEG_{15}–Fab_{IL6R} was observed for both VEGF and IL6R (ESI,† Fig. S9). The kinetic rate constants and affinities were calculated (Table 3) using a 1 : 1 binding model.

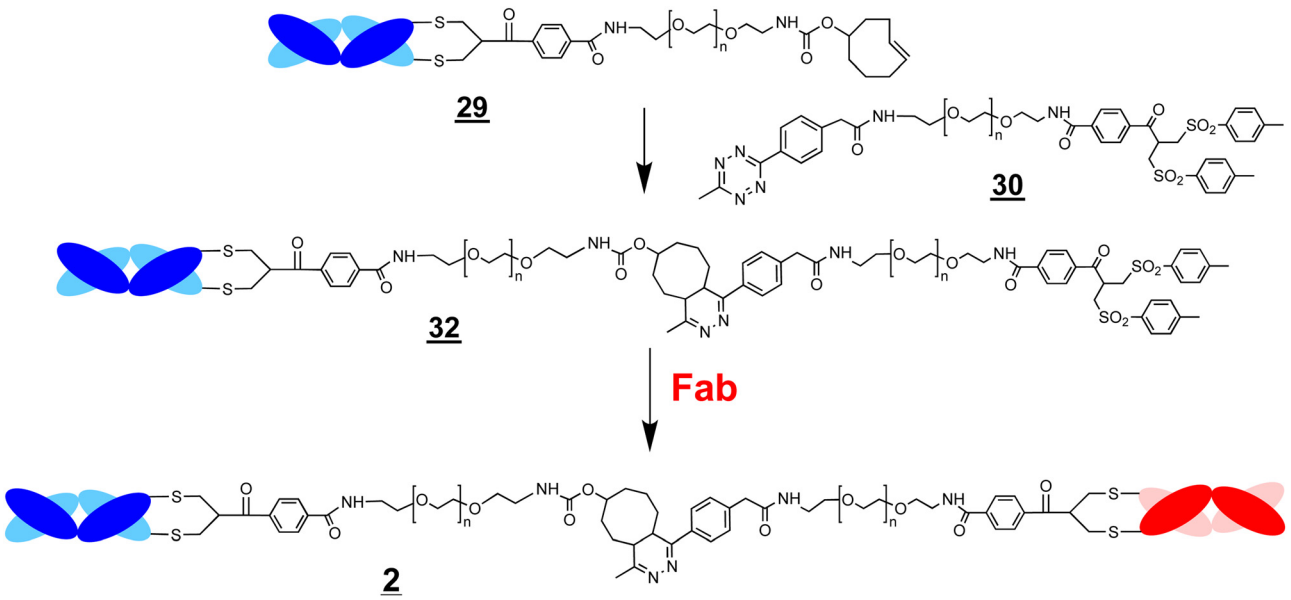

Scheme 7 A conjugation–ligation–conjugation strategy to prepare the bsFpF **2**. The Fab–PEG–TCO conjugate intermediate **29** undergoes ligation with the bis-sulfone–PEG–Tz reagent **30** to give the intermediate Fab–PEG–TCO **32**. A second Fab is then conjugated to the intermediate **36** to give the final bsFpF **2**.

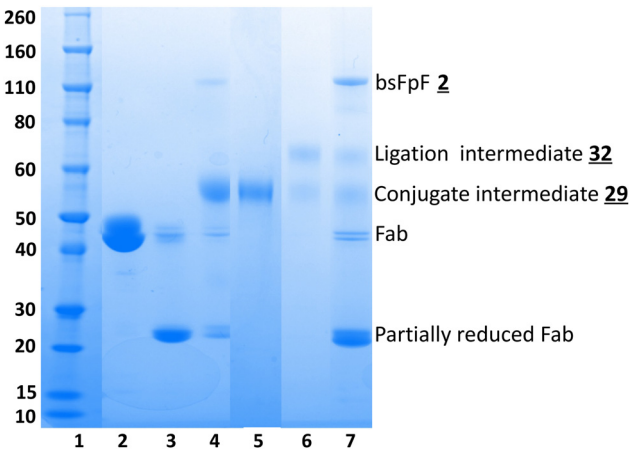

Fig. 4 The SDS–PAGE gel displaying preparation of a bsFpF **2** by conjugation–ligation–conjugation; Fab is first conjugated to bis-sulfone–PEG_{10}–TCO **28** to give the Fab–PEG_{10}–TCO conjugate intermediate **29** which is then ligated to bis-sulfone–PEG_5–Tz **30** to form the bis-sulfone terminated ligation intermediate **32** (note Scheme 7) which can undergo conjugation with another Fab to give the bsFpF. Lane 1: protein markers, lane 2: Fab_{VEGF}, lane 3: Fab_{VEGF} + DTT, lanes 4 and 5: conjugation of reduced Fab_{VEGF} to bis-sulfone–PEG_{10}–TCO **28**, and then purified, lane 6: Fab_{VEGF}–PEG_{10}–TCO ligation with bis-sulfone–PEG_5–Tz **30** to give the ligation intermediate **32** which then underwent conjugation with reduced Fab_{IL6R} in lane 7: resulting in the formation of the Fab_{VEGF}–PEG_{15}–PEG_{IL6R} bispecific molecule.

ESI,† Table S1 summarises the SPR derived kinetic rate constants and affinities that were obtained for bsFpFs prepared by conjugation–ligation using the TCO and Tz bis-sulfone reagents **28** and **30**.

The homodimer FpF_{VEGF} prepared by the di(bis-sulfone) PEG reagent **3** appeared to have lower K_D due to a faster association rate (k_a) constant and a slower dissociation rate (k_d) compared to the homodimer FpF_{VEGF} synthesised by a conjugation–ligation (reagents **28** and **30**) approach, studied by both ELISA and SPR (Fig. 6).

Immunoblotting (dot blot assays) is also useful for qualitative assessment of binding interactions; for example, Fab_{VEGF}–PEG_{15}–Fab_{COL2} displayed binding to its respective antigens using a dot blot assay (Fig. S10, ESI†). A limitation of ELISA, SPR and dot blot assays is that these techniques require immobilisation of one of the binding partners which may not fully represent the dynamic interactions of the binding partners in solution.[47] Microscale thermophoresis (MST) enables the practical measurement of binding interactions in solution. Using MST, the binding analysis of bispecific Fab_{VEGF}–PEG_{15}–Fab_{IL6R} was performed on VEGF, IL6R and a mixture of VEGF/IL6R (Fig. S11, ESI†). The binding traces revealed that the bispecific Fab_{VEGF}–PEG_{15}–Fab_{IL6R} maintained its binding towards both VEGF and IL6R, both as individual targets and when presented as a mixed target (VEGF/IL6R) in solution.

Discussion

There is a rich history of investigating dimeric low molecular weight molecules and proteins linked by PEG, *e.g.*[48–51] As a dimeric antibody-based molecule, the FpF motif is a good IgG binding mimetic.[1,2] Each Fab is covalently bound to a terminus of a linear, flexible PEG in the region where the Fab is naturally anchored in an IgG. The PEG linker appears to mimic some of the conformational properties of the IgG hinge to allow flexible Fab–epitope interactions during binding, which are important for antibody functions.[3] FpFs evaluated to date appear to have comparable binding thermodynamics to the corresponding IgG

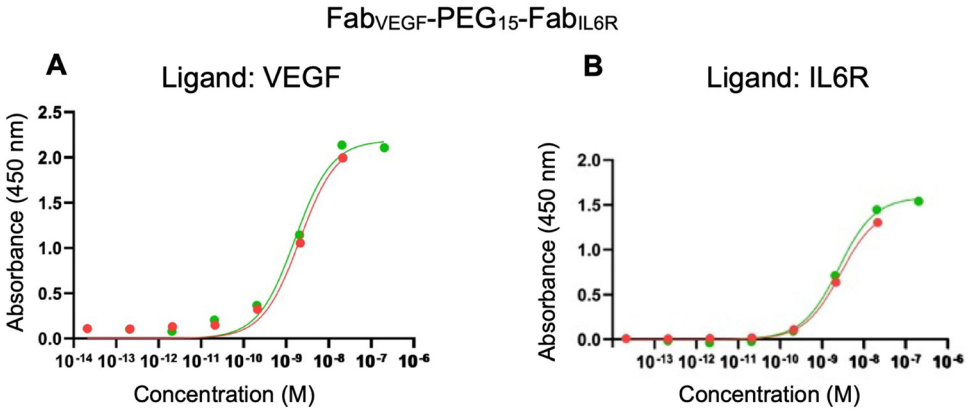

Fig. 5 ELISA results for (A) Fab_{VEGF}–PEG_{15}–Fab_{IL6R} (green data point) and mono PEG–Fab_{VEGF} (red data point) with a concentration range of 1.3×10^{-7} to 1.3×10^{-13} M over wells coated with VEGF (0.1 μg). (B) Fab_{VEGF}–PEG_{15}–Fab_{IL6R} (green data point) and mono PEG–Fab_{IL6R} (red data point) with a concentration range of 1.3×10^{-7} to 1.3×10^{-13} M over wells coated with IL6R (0.1 μg).

Table 2 Binding affinities (K_D) for mono-PEG–Fabs and Fab_{VEGF}–PEG_{15}–Fab_{IL6R} against VEGF and IL6R using the ELISA technique

Conjugates	Ligand	K_D (nM)
PEG_{10}–Fab_{VEGF}	VEGF	2.25
Fab_{VEGF}–PEG_{15}–Fab_{IL6R}	VEGF	1.80
PEG_5–Fab_{IL6R}	IL6R	3.20
Fab_{VEGF}–PEG_{15}–Fab_{IL6R}	IL6R	2.55

antibody with the same Fabs.[1,2] FpF affinity is achieved by a slower association rate (k_a) that is then compensated by a correspondingly slower dissociation rate (k_d). A slower k_d may have important therapeutic potential to help maintain localised therapeutic concentrations in tissues.[52–54]

FpFs do not have the extended solution structure of a PEG–Fab conjugate where there is a protein only on one terminus of the PEG molecule.[1] FpFs appear to have a similar solution size to IgGs broadly independent on the PEG linker size in the range of 5–20 kDa.[1] It is thought that the Fab moieties in a FpF may self-associate to reduce the size of PEG in solution compared to what is observed for PEGylated proteins with a protein conjugated at only one PEG terminus. FpFs in solution may possess some of the conformational properties associated with A–B–A block copolymers[55,56] where the Fabs (A block) can self-associate. Since bsFpFs have a Fab at each terminus of a PEG molecule like the homo-dimeric FpFs, it would be expected that the bsFpFs will have a similar size to the homodimeric FpFs.

It will be important to examine the differences in the solution structures for the FpFs made by the conjugation-only approach and by the conjugation–ligation approach where there is a ligation element located within the PEG linker. Although binding appears broadly similar, the ligation elements may exert conformational influences (Fig. 6). It is also clear from other studies that the PEG linker length in dimeric protein conjugates can influence binding, especially below a threshold length that is shorter than the ligand or the epitope distance.[49,50,57] We recognise that there is also potential to optimise the bsFpF linker length depending on the specific application.

Since the IgG hinge region is susceptible to degradation, the use of a PEG linker and site-specific bis-alkylation conjugation at the accessible Fab disulfide contribute to the stability and reduced propensity for aggregation of FpFs.[1] The thiol–ether bonds conjugating each Fab to the flexible PEG linker acting as the surrogate hinge are more stable than the unmodified accessible disulfide in the Fab. Much effort remains focused on developing antibody-based molecules with optimal physicochemical properties,[58] some of which FpFs may have the potential to display.

Multifunctional protein conjugates including bispecific antibodies can be made using proteins that are readily accessible by recombinant means (*e.g.* Fabs and single chain fragments) which are then conjugated by selective chemical strategies. Outstanding studies have been published exemplifying this approach,[35,59–61] including strategies to conjugate proteins or peptides at each terminus of a functionalised PEG linker analogous to what we have described for FpFs.[9,10,62] FpFs comprise elements (*e.g.* Fabs and PEG) which separately have been clinically proven viable for use.

Table 3 Average kinetic constant rates of mono-PEG–Fabs and Fab_{VEGF}–PEG_{15}–Fab_{IL6R} (N = 3) using the 1 : 1 binding model. Chi^2 values, a fitting quantitative measure, were 0.12 for Fab_{VEGF}–PEG_{15}–Fab_{IL6R} and 0.52 for mono-PEG–Fabs. The optimal Chi^2 value is within a 10% range of the R_{max} value

Conjugates	Ligand	k_a (1/Ms) $\times 10^4$	SD $k_a \times 10^4$	k_d (1/s) $\times 10^{-4}$	SD $k_d \times 10^{-4}$	K_D (nM)	SD K_D
PEG_{10}–Fab_{VEGF}	VEGF	1.30	0.06	1.4	0.35	10.9	3.0
Fab_{VEGF}–PEG_{15}–Fab_{IL6R}	VEGF	0.84	0.31	1.0	0.4	12	7.8
PEG_5–Fab_{IL6R}	IL6R	3.90	1.83	12.5	4.94	38.1	29.6
Fab_{VEGF}–PEG_{15}–Fab_{IL6R}	IL6R	2.80	1.30	5.7	0.56	23.3	14.4

A

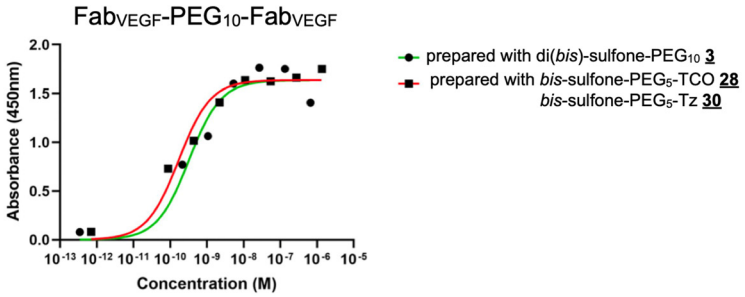

B

Fab$_{VEGF}$-PEG$_{10}$-Fab$_{VEGF}$

Reagents used	ka (1/Ms) x10^4	kd (1/s) x10^{-5}	K_D (nM)
di(*bis*)-sulfone-PEG$_{10}$ **3**	1.9	3.0	1.5
bis-sulfone-PEG$_5$-TCO **28** *bis*-sulfone-PEG$_5$-Tz **30**	0.7	5.1	7.0

Fig. 6 Binding analysis of the homodimer FpF$_{VEGF}$ prepared using the conjugation reagent **3** and conjugation–ligation reagents **28** and **30** using (A) ELISA, plate coated with VEGF$_{165}$ (0.1 μg) and (B) SPR technique, and the CM3 chip immobilised with VEGF (95 RU).

The di(bis-sulfone) reagent **3** was examined to prepare the heterodimeric bsFpFs **2** because this is an effective reagent to prepare the homodimeric FpFs **1**. We anticipated that conjugation of the first Fab to the di(bis-sulfone) **3** would be faster than the second Fab due to possible hydrophilic steric shielding effects of the second bis-sulfone conjugation moiety after conjugation of Fab$_1$. Modification of the leaving groups in the bis-sulfone conjugation moiety to increase hydrophilicity was considered,[63] although an excess reagent would still be required for the first conjugation step in a conjugation-only approach with a di(bis-sulfone) reagent. The addition of excess di(bis-sulfone) **3** during the conjugation of Fab$_1$ predominantly gave the desired Fab$_1$–PEG–bis sulfone **4** intermediate (***e.g.*** Fab$_{VEGF}$–PEG$_{10}$–bis-sulfone **4**, Fig. 1A). The use of excess di(bis-sulfone) **3** necessitates its removal prior to the conjugation of Fab$_2$. Ion exchange chromatography (IEX) effectively removed the excess reagent along with trace remaining Fab$_1$ and the homodimer (*i.e.* Fab$_1$–PEG–Fab$_1$).

Conjugation of Fab$_2$ required longer incubation times (Fig. 1B), which may not be ideal for maintaining Fab$_2$ stability and preventing reoxidation of the Fab$_2$ accessible disulfide. The di(bis)-sulfone **3** was purified by precipitation,[64] which works well for reagents designed to undergo a single conjugation reaction, *e.g.* bis-sulfone PEGylation reagents **5** (Fig. 1C).[65] The use of pure PEG precursors and the chromatographic purification of the di(bis-sulfone) **3** does give a reagent with less possible dead chain ends (Fig. S1, ESI†)[9] and does appear more effective for the second conjugation step (Fig. 1A, lane 8). Although we are keen to utilise reagents that could be prepared without a tedious purification to isolate the reagent, it is important to acknowledge that minimisation of dead chain ends in all conjugation reagents is generally preferred.

The asymmetric FpF reagents **16** (Schemes 3 and 4) indicate that we could reduce the excess of the reagent needed for the conjugation of Fab$_1$ and reduce the formation of the undesired homodimer. The fluoro-substituted bis-sulfide conjugation moieties are less reactive than the bis-sulfone conjugation moiety; however, all these bis-alkylation moieties yield the same conjugate product (*e.g.* PEG–Fab **6**, compare Fig. 1C and 2A). There are few if any di-conjugation reagents that undergo the same site-specific conjugation reaction at each moiety but with varied reactivity.

Our preliminary experiments indicated that the combination of reduced reactivity for the bis-sulfide conjugation moiety for Fab$_2$ and the reduced reaction rate for the second conjugation to the Fab–PEG–bis-sulfide intermediate **17** (Scheme 4) meant that there was often remaining Fab$_2$ present with the conditions that were examined. Considering the advantages of a cleaner reaction for Fab$_1$, more work is required to optimise the conjugation of the second protein (*e.g.* Fab$_2$).

The ligation approach to prepare bsFpFs is to utilise bis-alkylation conjugation that site-specifically rebridges the two cysteine thiols from the accessible native disulfide of a Fab to give conjugate intermediates that are then ligated *via* an orthogonal cycloaddition reaction. Many ligation strategies have been described (*e.g.* ref. 66–68). Ligations are often accomplished by orthogonal reactions (*e.g.* ref. 69), with cycloaddition reactions dominating in recent years (*e.g.* ref. 45, 46 and 68) to make multifunctional proteins including bispecific antibody mimetics.[35,45] Protein modification strategies involving conjugation and/or ligation will inevitably evolve in the context of engineering protein structure recombinantly to best match a given modification strategy. Although our use of reagents with PEG molecular weights greater than 3 kDa is designed to yield bsFpFs that can be optimised to exploit spatial–temporal relationships that exist with IgGs, the use of these relatively long PEG linkers may also result in conjugation intermediates (*e.g.* Fab–PEG$_{10}$–TCO, Fab–PEG$_5$–Tz) that have

reduced ligation reactivity due to conformational masking of the ligation moiety.

Conjugation–ligation (Scheme 6) allows for a combinatorial approach to prepare bsFpFs **2**. For example, one conjugate intermediate (*e.g.* **29**) could undergo ligation with many different versions of its partner conjugate intermediate (*e.g.* **31**) to give a small family of bsFpFs **2**. Reaction orthogonality to the protein in the ligation step also reduces the potential for non-selective protein conjugation which is possible by the conjugation only approach when longer incubation times are used (*e.g.* >1 day). A conjugation–ligation approach also avoids generation of homo-dimeric protein conjugates that can result from a conjugation only approach, minimising the number of protein conjugation reactions needed and the need to purify bsFpFs from the unmodified protein.

Ligation using *trans*-cyclooctene (TCO) and tetrazine (Tz) moieties is faster than the cycloaddition between azide and DBCO moieties.[42,43,70] Bis sulfone–PEG–TCO **28** and bis sulfone–PEG–Tz **30** were prepared and used to make several bsFpFs **2** (Scheme 6) that were isolated (Fig. 3 and Table 1). We found that the isolated yields of purified proteins modified by different thiol specific conjugation strategies at a small scale (~0.5 to 2.0 mg) often give moderate to low yields due to the loss of protein during purification.[71,72] It is possible with high conversion that disulfide rebridging PEGylation reactions at these or slightly higher scales give isolated yields of 45–65% of the modified protein (*e.g.* ref. 40). Although the conjugation–ligation reagents **28** and **32** were precipitated 3–4 times during isolation (ESI†), additional chromatographic purification of the reagent (*e.g.* Fig. S1, ESI†) would be expected to increase overall conversion and isolated yields of the bsFpFs **2** at the scales we examined.

Challenges exist in the assay development of dual-targeting molecules.[73–76] Using Fab_{VEGF}–PEG_{15}–Fab_{IL6R} as a representative example, we examined the binding affinity by dot blot, ELISA, SPR and MST (Tables 2 and 3). The K_D value obtained from the binding assays varies across these different experiments (compare the K_D value for the same bsFpF molecule between Tables 2 and 3). ELISA experiments indicate each Fab in Fab_{VEGF}–PEG_{15}–Fab_{IL6R} has a similar affinity (K_D) as the corresponding PEG–Fab (Table 2). PEG conjugation reduces protein activity generally, and certainly Fab affinity compared to the unmodified Fab due to steric shielding effects of PEG. Disulfide-rebridging conjugation at the accessible Fab disulfide is near the region of the Fab that is connected to the hinge in a native IgG and is maximally distal to the complementarity-determining region (CDR) responsible for Fab binding to its respective target. Conjugation at this accessible disulfide is thought to cause less reduction in Fab affinity than conjugation elsewhere in the Fab.[1,40]

The binding kinetics to give the association (k_a) and dissociation (k_d) rate constants for three bsFpFs **2** determined by SPR are summarised in Table 3 and ESI,† Table S1. Low-density ligand immobilisation and a high flow rate (30 μL min^{-1}) were used to minimise mass transfer limitations and re-binding effects to the immobilised ligand.[77] Considering binding to immobilised $VEGF_{165}$, the apparent K_D and k_d values for mono-PEG_{10}–FabVEGF **6** (K_D 10.9 nM; k_d 1.4×10^{-4} 1/s) were similar to the bsFpFs **2** that with one Fab_{VEGF}; (i) Fab_{VEGF}–PEG_{15}–FabIL6R (K_D 12 nM and k_d 1.0×10^{-4} 1/s) (Table 3) and (ii) Fab_{VEGF}–PEG_{15}–$FabTNF_{\alpha}$ (K_D 10 nM and k_d 0.81×10^{-4} 1/s) (ESI,† Table S1).

We and others have previously shown that the dissociation rate constant of PEG modified Fabs remains broadly similar compared to the unmodified Fab.[40,78] This trend was also observed for the dissociation of Fab_{beva} in PEG_{10}–Fab_{beva}, and Fab_{VEGF}–PEG_{15}–Fab_{IL6R} from VEGF and Fab_{IL6R} in PEG_5–Fab_{IL6R} and Fab_{VEGF}–PEG_{15}–Fab_{IL6R} from IL6R. Similar trends in the dissociation rate constants were observed for Fab_{VEGF}–PEG_{10}–Fab_{HER2} prepared using the PEG di(bis-sulfone) reagent **3** (Fig. 1D). The data indicate that there was a little difference between the dissociation rate constants for Fab_{VEGF}, PEG_{10}–Fab_{VEGF} and Fab_{VEGF}–PEG_{10}–$Fab_{Her\text{-}2}$ conjugates (Fig. 1D). There is potential that the preparation of PEG–Fab_1 will be a good surrogate for the binding of Fab_1 in the corresponding bsFpF (*i.e.* Fab_1–PEG–Fab_2).

The association rate constants (k_a) were smaller for the FabVEGF–PEG_{15}–FabIL6R products to both immobilised VEGF and IL6R compared to the corresponding mono-PEG–Fab constructs (Table 3). The association rate constant of Fab_{VEGF}–PEG_{15}–Fab_{IL6R} is slower probably because the bsFpF is larger in molecular weight than a PEG–Fab which results in a slower rate of transport from bulk solution to the chip surface. A similar trend was observed for Fab_{VEGF}–PEG_{10}–Fab_{HER2} to have a slower association rate constant compared to PEG_{10}–Fab_{VEGF}. Reduction in binding affinities (K_D) for Fab conjugates compared to the corresponding unmodified Fab tends to be due to reductions in the association rate constants (k_a).[1,40,78] All bsFpFs molecules have a larger mass than PEG_{10}–Fab conjugates which results in a slower rate of transport over the chip surface.

ELISA, SPR and dot blot techniques are useful to confirm the binding of each Fab element in a bsFpF **2** but immobilisation of binding targets is required on a chip or the surface of a plate. Such assays do not fully replicate the dynamic nature of *in vivo* interactions where the binding partners interact in solution while moving freely.[79,80] Isothermal calorimetry can be used to evaluate binding properties in solution, but MST is also a real-time, solution-based method to measure binding interactions. MST requires that one protein be non-specifically labelled with a fluorescent dye. We elected to label the bsFpF in these experiments to utilise the same labelled molecule to evaluate both binding moieties in the bsFpF. Using MST, the binding analysis of bispecific Fab_{VEGF}–PEG_{15}–Fab_{IL6R} was performed on VEGF, IL6R and a mixture of VEGF/IL6R (Fig. S11A–C, ESI†). MST binding curves can appear in both directions as observed in Fig. S11A–C (ESI†) depending on the diffusion coefficients of the labelled protein and complex.[81] The binding curves indicate that the bispecific Fab_{VEGF}–PEG_{15}–Fab_{IL6R} maintained its binding towards both VEGF and IL6R separately and as a mixture.

To consider the presence of the ligation element in the PEG linker, we evaluated a homodimer FpF_{VEGF} prepared by PEG

di(bis)-sulfone **3** and homodimer FpF_{VEGF} prepared by conjugation–ligation (reagents **28** and **30**). While the dissociation rate constant (k_d) appeared broadly similar, the binding affinity (K_D) was smaller for the FpF_{VEGF} prepared by the ligation approach (Fig. 6). The lower binding affinity for the ligated FpF_{VEGF} appears to be due to a slightly slower association rate constant (k_a). The ligation element may slightly restrict the freedom for the association of the second Fab to the immobilised ligand. It will be worthwhile to explore the conformational influences of the presence and absence of the ligation element, specifically with the PEG linker molecular weight.

A range of bispecific FpFs targeting different antigen epitopes with therapeutic properties for pro-inflammatory targets (tumour necrosis factor alpha or TNF-α, interleukins 6R, and interleukins17) and a pro-angiogenic target (vascular endothelial growth factor or VEGF) were prepared. We also explored the preparation of 2 bsFpFs, Fab_{VEGF}–PEG–Fab_{HA} and Fab_{VEGF}–PEG–Fab_{COL2} where one Fab functions to bind to a specific non-therapeutic tissue (affinity targeting) and the other Fab functions to bind to a therapeutic target. Hyaluronic acid (HA) and collagen-II (COL2) are two endogenous tissue targets that are envisaged for increasing the biological residence time of a molecule within the vitreous cavity of the eye.[82–85] If the relevant Fab can be sourced, then bsFpFs may have utility as bispecific antibody mimetics for early preclinical studies designed to explore new therapeutic strategies.

Conclusions

FpFs are IgG mimetics with the potential to act as IgG surrogates in a range of applications.[1] Bispecific FpFs were prepared as possible mimetics of bispecific IgGs. Although each element of the bsFpF (*e.g.* Fab and PEG linker) has been used clinically or can be sourced (*e.g.* Fab_{COL2} and Fab_{HA}), the potential of bsFpFs may be in preclinical research to develop strategies for (i) drug delivery where one Fab targets a specific anchor point (*e.g.* hyaluronic acid or collagen II in the vitreous cavity of the eye) to achieve the enhanced residence time in the tissue or organ of interest, (ii) tissue regeneration where one moiety would bind to a scaffold[86–88] while the other moiety would provide a required biological function or for cell immobilisation[89] and (iii) drug target development to optimise the spatial–temporal aspects[90,91] of binding kinetics of a bispecific antibody and where it is not possible to use multiple antibodies in a single dosage form (*e.g.* intraocular indications).

Data availability

The data supporting this article have been included as part of the ESI.†

Conflicts of interest

There are no conflicts to declare.

Acknowledgements

M. C. is thankful for the PhD funding from the University of East London. N. I. is grateful for the PhD funding from the Santen Pharmaceutical Co., Ltd. W. R. G is thankful for the VC PhD scholarship from the University of West London. S. A., P. T. K., and S. B. are grateful for the funding from the National Institute of Health Research (NIHR) Biomedical Research Centre at Moorfields Eye Hospital NHS Foundation Trust and UCL Institute of Ophthalmology, the Helen Hamlyn Trust (in memory of Paul Hamlyn), Moorfields Eye Charity, Fight for Sight, and the Michael and Ilse Katz foundation.

References

1 H. Khalili, P. Khaw, R. Lever, A. Godwin and S. Brocchini, Fab-PEG-Fab as a potential antibody mimetic, *Bioconjugate Chem.*, 2013, **24**(11), 1870–1882.
2 H. Khalili, R. Lee, P. Khaw, S. Brocchini and A. Dick, An anti-TNF alpha antibody mimetic to treat ocular inflammation, *Sci. Rep.*, 2016, **6**, 36905.
3 R. Nezlin, Dynamic Aspects of the Immunoglobulin Structure, *Immunol. Invest.*, 2019, **48**(8), 771–780.
4 L. Harris, S. Larson, E. Skaletsky and A. McPherson, Comparison of the conformations of two intact monoclonal antibodies with hinges, *Immunol. Rev.*, 1998, **163**, 35–43.
5 I. R. Correia, Stability of IgG isotopes in serum, *mAbs*, 2010, **2**, 221–232.
6 H. Khalili, Using different proteolytic enzymes to digest antibody and its impact on stability of antibody mimetics, *J. Immunol. Methods*, 2021, **489**, 112933.
7 S. Brocchini, S. Balan, A. Godwin, J.-W. Choi, M. Zloh and S. Shaunak, PEGylation of native disulfide bonds in proteins, *Nat. Protoc.*, 2006, **1**(5), 2241–2252.
8 S. Balan, J. W. Choi, A. Godwin, I. Teo, C. M. Laborde, S. Heidelberger, M. Zloh, S. Shaunak and S. Brocchini, Site-specific PEGylation of protein disulfide bonds using a three-carbon bridge, *Bioconjugate Chem.*, 2007, **18**(1), 61–76.
9 A. Herrington-Symes, J. Choi and S. Brocchini, Interferon dimers: IFN-PEG-IFN, *J. Drug Targeting*, 2017, **25**(9–10), 881–890.
10 H. Khalili, P. Khaw and S. Brocchini, Fc-fusion mimetics, *Biomater. Sci.*, 2016, **4**(6), 943–947.
11 S. E. Sedykh, V. V. Prinz, V. N. Buneva and G. A. Nevinsky, Bispecific antibodies: design, therapy, perspectives, *Drug Des., Dev. Ther.*, 2018, **12**, 195–208.
12 U. Brinkmann and R. E. Kontermann, The making of bispecific antibodies, *mAbs*, 2017, **9**(2), 182–212.
13 D. Nagorsen, P. Kufer, P. A. Baeuerle and R. Bargou, Blinatumomab: A historical perspective, *Pharmacol. Ther.*, 2012, **136**(3), 334–342.
14 E. Wolf, R. Hofmeister, P. Kufer, B. Schlereth and P. A. Baeuerle, BiTEs: bispecific antibody constructs with unique anti-tumor activity, *Drug Discovery Today*, 2005, **10**(18), 1237–1244.

15 H. Shim, Bispecific Antibodies and Antibody-Drug Conjugates for Cancer Therapy: Technological Considerations, *Biomolecules*, 2020, **10**(3), 360.
16 S. W. Pipe, M. Shima, M. Lehle, A. Shapiro, S. Chebon, K. Fukutake, N. S. Key, A. Portron, C. Schmitt, M. Podolak-Dawidziak, N. S. Bienz, C. Hermans, A. Campinha-Bacote, A. Kiialainen, K. Peerlinck, G. G. Levy and V. Jiménez-Yuste, Efficacy, safety, and pharmacokinetics of emicizumab prophylaxis given every 4 weeks in people with haemophilia A (HAVEN 4): a multicentre, open-label, non-randomised phase 3 study, *Lancet Haematology*, 2019, **6**(6), E295–E305.
17 M. Collins, S. Awwad, N. Ibeanu, P. T. Khaw, D. Guiliano, S. Brocchini and H. Khalili, Dual-acting therapeutic proteins for intraocular use, *Drug Discovery Today*, 2021, **26**(1), 44–55.
18 T. Hansel, H. Kropshofer, T. Singer, J. Mitchell and A. George, The safety and side effects of monoclonal antibodies, *Nat. Rev. Drug Discovery*, 2010, **9**, 325–338.
19 P. Mayes, K. Hance and A. Hoos, The promise and challenges of immune agonist antibody development in cancer, *Nat. Rev. Drug Discovery*, 2018, **17**, 509–527.
20 G. Riethmuller, Symmetry breaking: bispecific antibodies, the beginnings, and 50 years on, *Cancer Immun.*, 2012, **12**, 12.
21 M. Brennan, P. F. Davison and H. Paulus, Preparation of bispecific antibodies by chemical recombination of monoclonal immunoglobulin-G1 fragments, *Science*, 1985, **229**(4708), 81–83.
22 U. D. Staerz, O. Kanagawa and M. J. Bevan, Hybrid antibodies can target sites for attack by t-cells, *Nature*, 1985, **314**(6012), 628–631.
23 M. J. Glennie, H. M. McBride, A. T. Worth and G. T. Stevenson, Preparation and performance of bispecific F(ab'-gamma)2 antibody containing thioether-linked Fab'-gamma fragments, *J. Immunol.*, 1987, **139**(7), 2367–2375.
24 M. Surowka, W. Schaefer and C. Klein, Ten years in the making: application of CrossMab technology for the development of therapeutic bispecific antibodies and antibody fusion proteins, *mAbs*, 2021, **13**(1), 1967714.
25 S. Dickopf, G. J. Georges and U. Brinkmann, Format and geometries matter: Structure-based design defines the functionality of bispecific antibodies, *Comput. Struct. Biotechnol. J.*, 2020, **18**, 1221–1227.
26 T. Hofmann, S. Krah, C. Sellmann, S. Zielonka and A. Doerner, Greatest Hits-Innovative Technologies for High Throughput Identification of Bispecific Antibodies, *Int. J. Mol. Sci.*, 2020, **21**(18), 6551.
27 J. Steinhardt, Y. Wu, R. Fleming, B. T. Ruddle, P. Patel, H. Wu, C. Gao and N. Dimasi, Fab-Arm Exchange Combined with Selective Protein A Purification Results in a Platform for Rapid Preparation of Monovalent Bispecific Antibodies Directly from Culture Media, *Pharmaceutics*, 2020, **12**, 1.
28 L. Qian, X. Lin, X. Gao, R. U. Khan, J.-Y. Liao, S. Du, J. Ge, S. Zeng and S. Q. Q. Yao, The Dawn of a New Era: Targeting the ''Undruggables'' with Antibody-Based Therapeutics, *Chem. Rev.*, 2023, **123**(12), 7782–7853.
29 O. Harel and M. Jbara, Chemical Synthesis of Bioactive Proteins, *Angew. Chem., Int. Ed.*, 2023, **62**(13), e202217716.
30 L. Xu, S. L. Kuan and T. Weil, Contemporary Approaches for Site-Selective Dual Functionalization of Proteins, *Angew. Chem., Int. Ed.*, 2021, **60**(25), 13757–13777.
31 R. J. Taylor, M. B. Geeson, T. Journeaux and G. J. L. Bernardes, Chemical and Enzymatic Methods for Post-Translational Protein-Protein Conjugation, *J. Am. Chem. Soc.*, 2022, **144**(32), 14404–14419.
32 S. C. Lee, J. S. Y. Ma, M. S. Kim, E. Laborda, S. Choi, E. N. Hampton, H. Yun, V. Nunez, M. T. Muldong, C. N. Wu, W. Ma, A. A. Kulidjian, C. J. Kane, V. Klyushnichenko, A. K. Woods, S. B. Joseph, M. Petrassi, J. Wisler, J. Li, C. A. M. Jamieson, P. G. Schultz, C. H. Kim and T. S. Young, A PSMA-targeted bispecific antibody for prostate cancer driven by a small-molecule targeting ligand, *Sci. Adv.*, 2021, **7**(33), eabi8193.
33 B. M. Hutchins, S. A. Kazane, K. Staflin, J. S. Forsyth, B. Felding-Habermann, V. V. Smider and P. G. Schultz, Selective Formation of Covalent Protein Heterodimers with an Unnatural Amino Acid, *Chem. Biol.*, 2011, **18**(3), 299–303.
34 H. Y. Liu, P. Zrazhevskiy and X. Gao, Solid-Phase Bioconjugation of Heterobifunctional Adaptors for Versatile Assembly of Bispecific Targeting Ligands, *Bioconjugate Chem.*, 2014, **25**(8), 1511–1516.
35 F. Thoreau, P. A. Szijj, M. K. Greene, L. N. C. Rochet, I. A. Thanasi, J. K. Blayney, A. Maruani, J. R. Baker, C. J. Scott and V. Chudasama, Modular Chemical Construction of IgG-like Mono- and Bispecific Synthetic Antibodies (SynAbs), *ACS Cent. Sci.*, 2023, **9**(3), 476–487.
36 S. Kishimoto, Y. Nakashimada, R. Yokota, T. Hatanaka, M. Adachi and Y. Ito, Site-Specific Chemical Conjugation of Antibodies by Using Affinity Peptide for the Development of Therapeutic Antibody Format, *Bioconjugate Chem.*, 2019, **30**(3), 698–702.
37 S. J. Walsh, J. D. Bargh, F. M. Dannheim, A. R. Hanby, H. Seki, A. J. Counsell, X. X. Ou, E. Fowler, N. Ashman, Y. Takada, A. Isidro-Llobet, J. S. Parker, J. S. Carroll and D. R. Spring, Site-selective modification strategies in antibody-drug conjugates, *Chem. Soc. Rev.*, 2021, **50**(2), 1305–1353.
38 E. A. Hoyt, P. Cal, B. L. Oliveira and G. J. L. Bernardes, Contemporary approaches to site-selective protein modification. Nature Reviews, *Chemistry*, 2019, **3**(3), 147–171.
39 M. Collins and H. Khalili, Soluble Papain to Digest Monoclonal Antibodies; Time and Cost-Effective Method to Obtain Fab Fragment, *Bioengineering*, 2022, **9**(5), 209.
40 H. Khalili, A. Godwin, J.-W. Choi, R. Lever and S. Brocchini, Comparative Binding of Disulfide-Bridged PEG-Fabs., *Bioconjugate Chem.*, 2012, **23**(11), 2262–2277.
41 M. Handula, K.-T. Chen and Y. Seimbille, IEDDA: An Attractive Bioorthogonal Reaction for Biomedical Applications, *Molecules*, 2021, **26**(15), 4640.
42 J. C. Jewett and C. R. Bertozzi, Cu-free click cycloaddition reactions in chemical biology, *Chem. Soc. Rev.*, 2010, **39**(4), 1272–1279.

43 K. Johann, D. Svatunek, C. Seidl, S. Rizzelli, T. A. Bauer, L. Braun, K. Koynov, H. Mikula and M. Barz, Tetrazine- and trans-cyclooctene-functionatised potypept(o)ides for fast bioorthogonal tetrazine ligation, *Polym. Chem.*, 2020, **11**(27), 4396–4407.
44 C. Ginn, J. Choi and S. Brocchini, Disulfide-bridging PEGylation during refolding for the more efficient production of modified proteins, *Biotechnol. J.*, 2016, **11**(8), 1088–1099.
45 L. Bartels, H. L. Ploegh, H. Spits and K. Wagner, Preparation of bispecific antibody-protein adducts by site-specific chemo-enzymatic conjugation, *Methods*, 2019, **154**, 93–101.
46 A. Battigelli, B. Almeida and A. Shukla, Recent Advances in Bioorthogonal Click Chemistry for Biomedical Applications, *Bioconjugate Chem.*, 2022, **33**(2), 263–271.
47 Y. Tang, X. Zeng and J. Liang, Surface Plasmon Resonance: An Introduction to a Surface Spectroscopy Technique, *J. Chem. Educ.*, 2010, **87**(7), 742–746.
48 V. M. Krishnamurthy, V. Semetey, P. J. Bracher, N. Shen and G. M. Whitesides, Dependence of effective molarity on linker length for an intramolecular protein-ligand system, *J. Am. Chem. Soc.*, 2007, **129**(5), 1312–1320.
49 R. Das, E. Baird, S. Allen, B. Baird, D. Holowka and B. Goldstein, Binding mechanisms of PEGylated ligands reveal multiple effects of the PEG scaffold, *Biochemistry*, 2008, **47**(3), 1017–1030.
50 R. H. Kramer and J. W. Karpen, Spanning binding sites on allosteric proteins with polymer-linked ligand dimers, *Nature*, 1998, **395**(6703), 710–713.
51 S. Kubetzko, E. Balic, R. Waibel, U. Z. Wittke and A. Pluckthun, PEGylation and multimeriztion of the anti-p185 HER-2 single chain Fv fragment 4D5, *J. Biol. Chem.*, 2006, **281**, 35186–35201.
52 G. Vauquelin and S. J. Charlton, Long-lasting target binding and rebinding as mechanisms to prolong in vivo drug action, *Br. J. Pharmacol.*, 2010, **161**(3), 488–508.
53 T. Ren, X. Zhu, N. M. Jusko, W. Krzyzanski and W. J. Jusko, Pharmacodynamic model of slow reversible binding and its applications in pharmacokinetic/pharmacodynamic modeling: review and tutorial, *J. Pharmacokinet. Pharmacodyn.*, 2022, **49**(5), 493–510.
54 J. Gabrielsson and S. Hjorth, Turn On, Tune In, Turnover! Target Biology Impacts In Vivo Potency, Efficacy, and Clearance, *Pharmacol. Rev.*, 2023, **75**(3), 416–462.
55 A. Halperin, Polymeric vs. monomeric amphiphiles: Design parameters, *Polym. Rev.*, 2006, **46**(2), 173–214.
56 H. Jung, S.-E. Gang, J.-M. Kim, T.-Y. Heo, S. Lee, E. Shin, B.-S. Kim and S.-H. Choi, Regulating Dynamics of Polyether-Based Triblock Copolymer Hydrogels by End-Block Hydrophobicity, *Macromolecules*, 2020, **53**(23), 10339–10348.
57 P. Pan, T. Geng, Z. Li, X. Ding, M. Shi, Y. Li, Y. Wang, Y. Shi, J. Wu, L. Zhong, D. Ji, Z. Li and X. Meng, Design, Synthesis, and Biological Evaluation of Proteolysis-Targeting Chimeras as Highly Selective and Efficient Degraders of Extracellular Signal-Regulated Kinase 5, *J. Med. Chem.*, 2023, **66**(19), 13568–13586.
58 H. L. Svilenov, P. Arosio, T. Menzen, P. Tessier and P. Sormanni, Approaches to expand the conventional toolbox for discovery and selection of antibodies with drug-like physicochemical properties, *mAbs*, 2023, **15**(1), 2164459.
59 R. J. Taylor, M. A. Rangel, M. B. Geeson, P. Sormanni, M. Vendruscolo and G. J. L. Bernardes, p-Clamp-Mediated Homo- and Heterodimerization of Single-Domain Antibodies via Site-Specific Homobifunctional Conjugation, *J. Am. Chem. Soc.*, 2022, **144**(29), 13026–13031.
60 W.-C. Lo, S. K. Kawade, W.-H. Kuo, A. K. Adak and C.-C. Lin, Site-selective heterodimerization of antibody fragments for bispecific antibody complexes enabled by divinylpyrimidine reagent, *J. Chin. Chem. Soc.*, 2023, **70**(12), 2177.
61 P. Szijj and V. Chudasama, The renaissance of chemically generated bispecific antibodies, *Nat. Rev. Chem.*, 2021, **5**(2), 78–92.
62 C. Sun, J. L. Trevaskis, C. M. Jodka, S. Neravetla, P. Griffin, K. Xu, Y. Wang, D. G. Parkes, B. Forood and S. S. Ghosh, Bifunctional PEGylated Exenatide-Amylinomimetic Hybrids to Treat Metabolic Disorders: An Example of Long-Acting Dual Hormonal Therapeutics, *J. Med. Chem.*, 2013, **56**(22), 9328–9341.
63 A. Godwin, G. Badescu, M. Bird, P. Bryant, D. Morris and M. Frigerio, *Process for the conjugation of a peptide or protein with a reagent comprising a leaving group including a portion of PEG*, 2016, p. 188.
64 Y. Cong, E. Pawlisz, P. Bryant, S. Balan, E. Laurine, R. Tommasi, R. Singh, S. Dubey, K. Peciak, M. Bird, A. Sivasankar, J. Swierkosz, M. Muroni, S. Heidelberger, M. Farys, F. Khayrzad, J. Edwards, G. Badescu, I. Hodgson, C. Heise, S. Somavarapu, J. Liddell, K. Powell, M. Zloh, J.-W. Choi, A. Godwin and S. Brocchini, Site-Specific PEGylation at Histidine Tags., *Bioconjugate Chem.*, 2012, **23**(2), 248–263.
65 S. Brocchini, A. Godwin, S. Balan, J.-W. Choi, M. Zloh and S. Shaunak, Disulfide bridge based PEGylation of proteins., *Adv. Drug Delivery Rev.*, 2008, **60**(1), 3–12.
66 R. Pihl, Q. Zheng and Y. David, Nature-inspired protein ligation and its applications, *Nat. Rev. Chem.*, 2023, **7**(4), 234–255.
67 A. H. Keeble and M. Howarth, Power to the protein: enhancing and combining activities using the Spy toolbox, *Chem. Sci.*, 2020, **11**(28), 7281–7291.
68 C. Schindler, C. Faust, H. Sjuts, C. Lange, J. Kuehn, W. Dittrich, W. D. Leuschner, W. Schiebler, J. Hofmann, E. Rao and T. Langer, A multivalent antibody assembled from different building blocks using tag/catcher systems: a case study, *Protein Eng., Des. Sel.*, 2022, **35**, gzac014.
69 E. M. Sletten and C. R. Bertozzi, Bioorthogonal Chemistry: Fishing for Selectivity in a Sea of Functionality, *Angew. Chem., Int. Ed.*, 2009, **48**(38), 6974–6998.
70 T. Reiner and B. M. Zeglis, The inverse electron demand Diels-Alder click reaction in radiochemistry, *J. Labelled Compd. Radiopharm.*, 2014, **57**(4), 285–290.
71 K. Muneeruddin, C. E. Bobst, R. Frenkel, D. Houde, I. Turyan, Z. Sosic and I. A. Kaltashov, Characterization of a PEGylated protein therapeutic by ion exchange

chromatography with on-line detection by native ESI MS and MS/MS, *Analyst*, 2017, **142**(2), 336–344.

72 J. E. Seely and C. W. Richey, Use of ion-exchange chromatography and hydrophobic interaction chromatography in the preparation and recovery of polyethylene glycol-linked proteins, *J. Chromatogr. A*, 2001, **908**(1–2), 235–241.

73 A. C. Register, S. S. Tarighat and H. Y. Lee, Bioassay Development for Bispecific Antibodies-Challenges and Opportunities, *Int. J. Mol. Sci.*, 2021, **22**(10), 5350.

74 M. Pei, Y. Wang, L. Tang, W. Wu, C. Wang and Y.-L. Chen, Dual-target Bridging ELISA for Bispecific Antibodies, *Bio-Protoc.*, 2022, **12**(19), e4522.

75 S. Mak, A. Marszal, N. Matscheko and U. Rant, Kinetic analysis of ternary and binary binding modes of the bispecific antibody emicizumab, *mAbs*, 2023, **15**(1), 2149053.

76 A. V. Madsen, O. Mejias-Gomez, L. E. Pedersen, K. Skovgaard, P. Kristensen and S. Goletz, Immobilization-Free Binding and Affinity Characterization of Higher Order Bispecific Antibody Complexes Using Size-Based Microfluidics, *Anal. Chem.*, 2022, **94**(40), 13652–13658.

77 A. Erbas and F. Inci, The Role of Ligand Rebinding and Facilitated Dissociation on the Characterization of Dissociation Rates by Surface Plasmon Resonance (SPR) and Benchmarking Performance Metrics, *Methods Mol. Biol.*, 2022, **2385**, 237–253.

78 S. Kubetzko, C. A. Sarkar and A. Plückthun, Protein PEGylation decreases observed target association rates via a dual blocking mechanism, *Mol. Pharmacol.*, 2005, **68**(5), 1439–1454.

79 A. Erbas, M. Olvera de la Cruz and J. F. Marko, Receptor-Ligand Rebinding Kinetics in Confinement, *Biophys. J.*, 2019, **116**(9), 1609–1624.

80 M. A. Cooper, Label-free screening of bio-molecular interactions, *Anal. Bioanal. Chem.*, 2003, **377**(5), 834–842.

81 M. Jerabek-Willemsen, T. Andre, R. Wanner, H. M. Roth, S. Duhr, P. Baaske and D. Breitsprecher, MicroScale Thermophoresis: Interaction analysis and beyond, *J. Mol. Struct.*, 2014, **1077**, 101–113.

82 J. G. Ghosh, A. A. Nguyen, C. E. Bigelow, S. Poor, Y. B. Qiu, N. Rangaswamy, R. Ornberg, B. Jackson, H. Mak, T. Ezell, V. Kenanova, E. de la Cruz, A. Carrion, B. Etemad-Gilbertson, R. G. Caro, K. Zhu, V. George, J. R. Bai, R. Sharma-Nahar, S. Y. Shen, Y. Q. Wang, K. K. Subramanian, E. Fassbender, M. Maker, S. Hanks, J. Vrouvlianis, B. Leehy, D. Long, M. Prentiss, V. Kansara, B. Jaffee, T. P. Dryja and M. Roguska, Long-acting protein drugs for the treatment of ocular diseases, *Nat. Commun.*, 2017, **8**, 14837.

83 M. Huelsmann and E. Kopetzki, *Fusion proteins for ophthalmology with increased eye retention*, 2017, p. 67.

84 F. E. Di Padova, J. Ghosh, T. Huber and J. R. Rondeau, *Compositions and methods for long-acting antibodies targeting IL-17*, 2015, p. 218.

85 M. Dang and M. S. Shoichet, Long-Acting Ocular Injectables: Are We Looking In The Right Direction? *Adv. Sci.*, 2024, **11**(8), 2306463.

86 K. Vulic and M. S. Shoichet, Affinity-Based Drug Delivery Systems for Tissue Repair and Regeneration, *Biomacromolecules*, 2014, **15**(11), 3867–3880.

87 M. Cai, L. Chen, T. Wang, Y. Liang, J. Zhao, X. Zhang, Z. Li and H. Wu, Hydrogel scaffolds in the treatment of spinal cord injury: a review, *Front. Neurosci.*, 2023, **17**, 1211066.

88 M. J. Kratochvil, A. J. Seymour, T. L. Li, S. P. Pasca, C. J. Kuo and S. C. Heilshorn, Engineered materials for organoid systems, *Nat. Rev. Mater.*, 2019, **4**(9), 606–622.

89 M. A. Kinney and T. C. McDevitt, Emerging strategies for spatiotemporal control of stem cell fate and morphogenesis, *Trends Biotechnol.*, 2013, **31**(2), 78–84.

90 J. W. Andrejecsk, W. G. Chang, J. S. Pober and W. M. Saltzman, Controlled protein delivery in the generation of microvascular networks, *Drug Delivery Transl. Res.*, 2015, **5**(2), 75–88.

91 J. E. Samorezov and E. Alsberg, Spatial regulation of controlled bioactive factor delivery for bone tissue engineering, *Adv. Drug Delivery Rev.*, 2015, **84**, 45–67.